inorganics

MDPI

Article

Synthesis, In Silico, In Vivo, and Ex Vivo Evaluation of a Boron-Containing Quinolinate Derivative with Presumptive Action on mGluRs

Mario Emilio Cuevas-Galindo [1], Brenda Anaid Rubio-Velázquez [1], Rosa Adriana Jarillo-Luna [2], Itzia I. Padilla-Martínez [3], Marvin A. Soriano-Ursúa [4,*] and José G. Trujillo-Ferrara [1,*]

[1] Departamento de Bioquímica, Sección de Estudios de Posgrado e Investigación, Escuela Superior de Medicina, Instituto Politécnico Nacional, Plan de San Luis y Díaz Mirón s/n, Col. Casco de Santo Tomás, Alc. Miguel Hidalgo, Mexico City 11340, Mexico
[2] Laboratorio de Morfología, Sección de Estudios de Posgrado e Investigación, Escuela Superior de Medicina, Instituto Politécnico Nacional, Plan de San Luis y Díaz Mirón s/n, Col. Casco de Santo Tomás, Alc. Miguel Hidalgo, Mexico City 11340, Mexico
[3] Laboratorio de Química Supramolecular y Nanociencias, Unidad Profesional Interdisciplinaria de Biotecnología, Instituto Politécnico Nacional, Av. Acueducto s/n, Col. La Laguna-Ticomán, Alc. Gustavo A. Madero, Mexico City 07340, Mexico
[4] Academia de Fisiología Humana y Sección de Estudios de Posgrado e Investigación, Escuela Superior de Medicina, Instituto Politécnico Nacional, Plan de San Luis y Díaz Mirón s/n, Col, Casco de Santo Tomás, lc. Miguel Hidalgo, Mexico City 11340, Mexico
* Correspondence: msoriano@ipn.mx (M.A.S.-U.); jtrujillo@ipn.mx (J.G.T.-F.); Tel.: +52-55-57296000 (ext. 62751) (M.A.S.-U.); +52-55-57296000 (ext. 62747) (J.G.T.-F.)

Abstract: In the brain, canonical excitatory neurotransmission is mediated by *L*-glutamate and its ionotropic (iGluR) and metabotropic (mGluR) receptors. The wide diversity of these often limits the development of glutamatergic drugs. This is due to the arduousness of achieving selectivity with specific ligands. In the present article, encouraged by reports of bioactive organoboron compounds, a diphenylboroxazolidone derived from quinolinate (*BZQuin*) was evaluated. *BZQuin* was synthesized with a yield of 87%. Its LD_{50} was 174 mg/kg in male CD-1 mice, as estimated by a modified Lorke's method. *BZQuin* exerted a reduced ability to cause seizures when compared against its precursor, quinolinate. The latter suggested that it does not directly stimulate the ionotropic NMDA receptors or other ionic channels. The observation that the antiglutamatergic drugs riluzole and memantine displaced the *BZQuin* effect left the mGluRs as their possible targets. This is in line with results from molecular-docking simulations. During these simulations, *BZQuin* bound only to orthosteric sites on mGluR1, mGluR2, and mGluR7, with higher affinity than quinolinate. The survival of the neurons of mice previously administered with *BZQuin* or quinolinate was quantified in four neuroanatomical structures of the brain. The *BZQuin* effect was more appreciable in brain regions with a high expression of the previously mentioned mGluRs, while both antiglutamatergic drugs exerted a neuroprotective effect against it. Together, these results suggest that *BZQuin* exerts a positive influence on glutamatergic neurotransmission while selectively interacting with certain mGluRs.

Keywords: quinolinate; organoboron; diphenylboroxazolidone; neurotransmission; glutamate receptor; seizures; histology; riluzole; memantine

Citation: Cuevas-Galindo, M.E.; Rubio-Velázquez, B.A.; Jarillo-Luna, R.A.; Padilla-Martínez, I.I.; Soriano-Ursúa, M.A.; Trujillo-Ferrara, J.G. Synthesis, In Silico, In Vivo, and Ex Vivo Evaluation of a Boron-Containing Quinolinate Derivative with Presumptive Action on mGluRs. *Inorganics* **2023**, *11*, 94. https://doi.org/10.3390/inorganics11030094

Academic Editor: Michael A. Beckett

Received: 24 January 2023
Revised: 24 February 2023
Accepted: 24 February 2023
Published: 26 February 2023

1. Introduction

One of the most prominent excitatory amino acids (EAAs) is *L*-glutamate. This neurotransmitter is involved in processes such as hyperexcitability, motor activity and skill, eyesight, the sense of pain, and long-term potentiation (LTP). With this is found a

persistent strengthening of the synapses, which play an important role in synaptic plasticity, and this is considered one of the main mechanisms behind learning and memory [1–3]. There exist two types of glutamate receptors on the cell membranes of presynaptic and postsynaptic neurons: ionotropic and metabotropic. These are the main targets for *L*-glutamate after its release into the synaptic cleft. The ionotropic glutamate receptors (iGluRs) are classified into three groups of ligand-gated cationic channels. These were identified pharmacologically and named after selective agonists that maintain a certain structural resemblance to *L*-glutamate and include the following: *α*-amino-3-hydroxy-5-methyl-4-isoxazole propionate (AMPA), *N*-methyl-*D*-aspartate (NMDA), and kainate receptors [1,2,4,5]. The metabotropic glutamate receptors (mGluRs) are G-protein-coupled receptors that are classified into the following three groups: I, II, and III [1,2,4,5].

As can be expected from this extensive family of receptors, *L*-glutamate is not the only ligand for them. There also exist other endogenous substances with affinities for these receptors, such as *D*-aspartate and quinolinate, an EAA and a metabolite of *L*-tryptophan, respectively. An increase in the presence of quinolinate and its positive influence on glutamatergic neurotransmission are often related with excitotoxicity, described as "a phenomenon whereby the excitatory action of *L*-glutamate and related EAAs becomes transformed into a neuropathological process that can rapidly kill central nervous system (CNS) neurons" [6]. This phenomenon is caused by an excess of *L*-glutamate, or some analogue, in the synaptic cleft. This is due to the inability of astrocytes to recapture it, which in turn gives rise to the overactivation of iGluRs and mGluRs, resulting in neurotoxicity [5,7].

In addition to the previously mentioned material, neuroinflammatory processes exert positive feedback on excitotoxicity and quinolinate biosynthesis. The latter is due to the presence of activated microglia and infiltrated macrophages in the CNS. These two types of immune cells possess the enzymatic machinery for the catabolism of *L*-tryptophan via the kynurenine pathway. This eventually leads to the harmful quinolinate concentrations often associated with neurological diseases, psychiatric disorders, and traumas or injuries. Under normal circumstances in the CNS, *L*-tryptophan is converted into the monoamine neurotransmitter 5-hydroxytryptamine (serotonin) and the sleep hormone 5-methoxy-*N*-acetyltryptamine (melatonin); low quinolinate concentrations allow its fast conversion into oxidized nicotinamide adenine dinucleotide (NAD+) [8–16]. In Figure 1, the canonical *L*-tryptophan metabolic pathway and its alternative kynurenine pathway are schematized.

The lack of a specific macromolecular target and the diverse mechanisms by which quinolinate exerts its neurotoxic effects are related to its structural resemblance to *D*-aspartate. Quinolinate is an NMDA receptor agonist, meaning that it activates the main iGluRs responsible for excitotoxicity. In addition, it promotes *L*-glutamate exocytosis into the synaptic cleft. This could be related to an interaction with group III mGluRs and could inhibit the glutamine synthetase enzyme in astrocytes [1,2]. In the brain, quinolinate at excitotoxic concentrations (500–1200 nM) can induce the expression of the nitric oxide synthase enzyme in neurons and astrocytes, as well as in proinflammatory cytokines, the most relevant of these being interleukin 1β (IL-1β) [14]. Additionally, it also disrupts the integrity of the blood–brain barrier (BBB), rendering it more permeable to different metabolites and drugs [14–16].

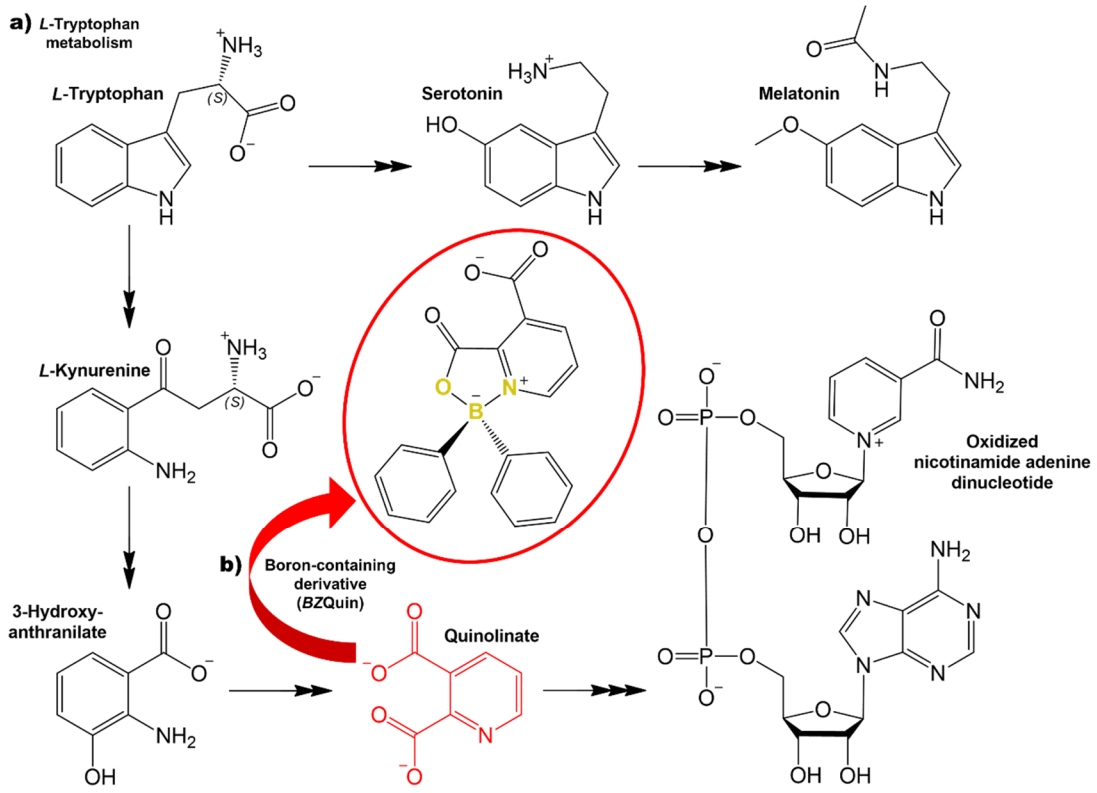

Figure 1. (**a**) *L*-Tryptophan metabolism: canonical pathway and kynurenine pathway. (**b**) *BZQuin* (yellow) heteroatoms forming a five-member heterocycle. The chemical structures are represented considering the protonation and deprotonation of their groups at physiological pH (7.4).

The synthesis of diphenylboroxazolidone from diphenylborinic acid and quinolinate (*BZQuin*) is encouraged. This is supported by evidence suggesting that boron-containing compounds exert effects on neuronal processes [17–20]. As early as the 18th century during the historical transition from alchemy to chemistry, sedative properties have been attributed to boron-containing salts. This is the case of Homberg sedative salt, whose main component is boric acid. The possible mechanism underlying these sedative properties may involve the direct interaction of boric acid with either voltage- or ligand-gated ionic channels. These channels represent the main mechanism through which some neurons execute fundamental electrophysiological events that enable interneural communication, which are known as action potentials. Ionic channels are responsible for the rapid depolarization and repolarization of these neurons, resulting in excitatory or inhibitory signals [21]. Currently, heterocyclic organoboron compounds that directly interact with ionic channels and are analogous to *BZQuin* have been fully identified. Such is the case of 2-aminoethyl diphenylborinate (2-APB), a five-member heterocycle derived from ethanolamine with a N→B bond. This negatively modulates the IP_3 receptors responsible for the release of Ca^{2+} from intracellular storage into the cytosol. Another precedent comprises a diphenylboroxazolidone derived from *L*-glutamate, which exerts an excitatory effect on *globus pallidus* neurons, as has been demonstrated by electrophysiological experiments. The observed excitatory effect is suggested to occur because of the possible interaction of the compound with the NMDA receptor, which has been simulated by molecular docking. In addition, from interactions with ionic channels, diphenylboroxazolidones derived from *L*-DOPA and *L*-tryptophan have been demonstrated to exert an ameliorative effect on murine models of Parkinson's and Alzheimer's diseases, respectively [22–27].

In the present work, the synthesis and evaluation by different means of the organoboron identified as *BZQuin* is presented. This is designed to take advantage of the already-known mechanisms and effects of quinolinate and organoboron analogues. Thus, from this is obtained a compound capable of exerting a positive influence on glutamatergic

neurotransmission, while selectively binding to a specific group of iGluRs or mGluRs. In Figure 1, the molecular structure of *BZQuin* is shown. In Figure 2, it is presented in comparison to those of the previously mentioned diphenylboroxazolidones and the excitatory quinolinate and *L*-glutamate analogues. Despite the similarity and analogy of their molecular structures, their selectivity for glutamate receptors may differ.

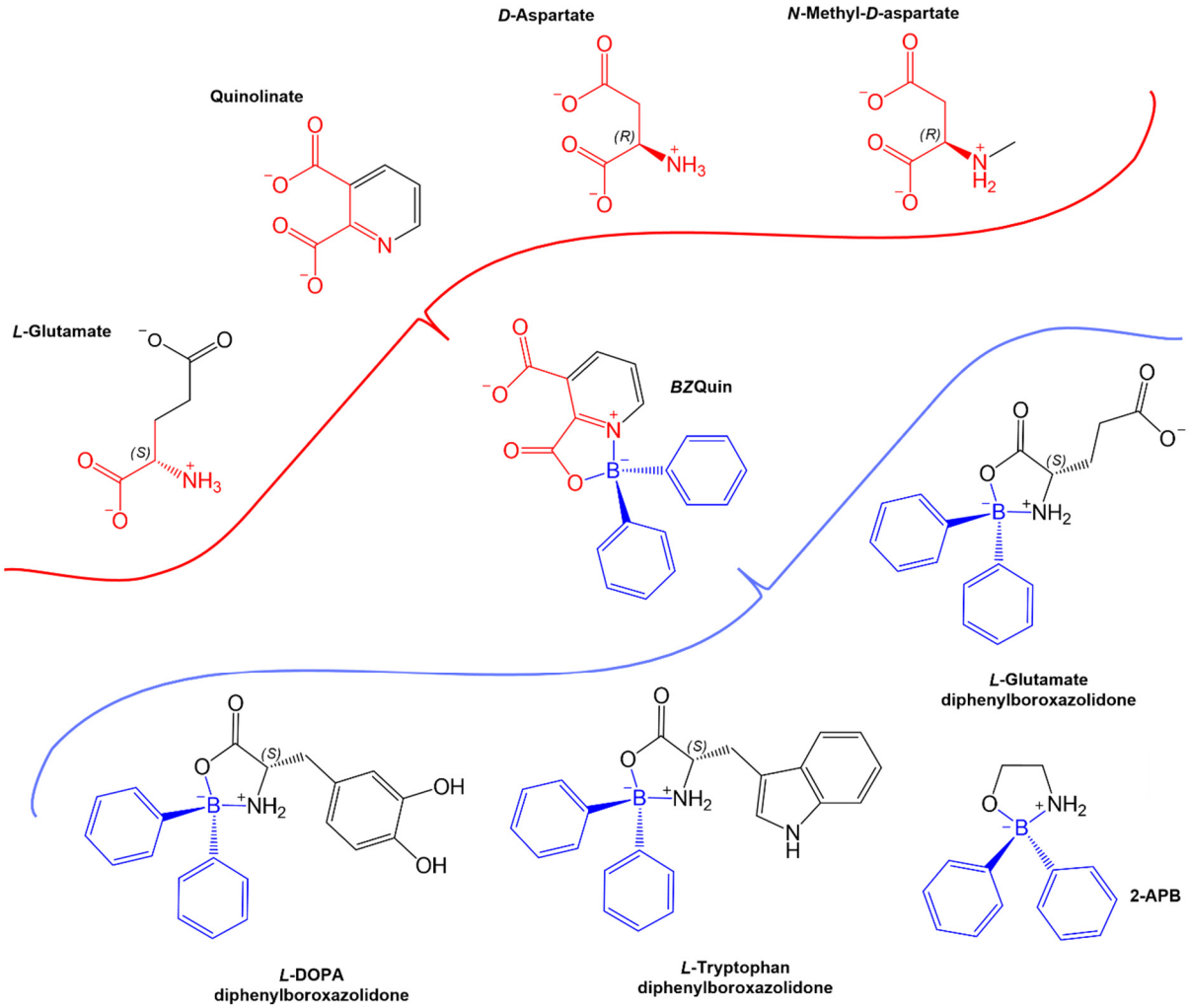

Figure 2. *BZQuin* structure comparison: (Red) EAA and quinolinate, which are iGluR and mGluR agonists; (Blue) diphenylboroxazolidones, which modify ionic channel activity or exert ameliorative effects on murine models of neurodegenerative diseases. The structural resemblances between *BZQuin* and both types of compounds are highlighted in their respective colors. The chemical structures are represented while considering protonation and deprotonation of their groups at physiological pH (7.4).

2. Results and Discussion

2.1. In Silico Evaluation: ADME Properties and Molecular Docking on Glutamate Receptors

The pharmacokinetic and physicochemical properties considered by the Lipinski Rule of Five, which were predicted with SwissADME for *BZQuin*, its precursor quinolinate (Quin), *L*-glutamate, and *D*-aspartate, are presented in Supplementary Table S1. It can be noted that the inhibition of the CYP2D6 or CYP3A4 cytochrome isoforms by *BZQuin* or by any of the evaluated molecules was not likely. Therefore, they might not interfere with drug metabolism in the liver. Aside from this, none of the analyzed molecules violated the Lipinski Rule of Five. Despite this, they were very hydrophilic, as can be observed from their MLOGP, which were mostly less than zero except for *BZQuin*.

This means that their passage through biological membranes could be compromised, especially for *L*-glutamate, *D*-aspartate, and to a lesser extent, Quin. It is also evident that, for *BZQuin*, the incorporation of the boron atom with the two phenyl rings improved its lipophilicity and gastrointestinal (GI) absorption, which is a desirable feature for enteric administration. This can be clearly observed in Supplementary Figure S1, which corresponds to the BOILED-Egg graph for the evaluated molecules. In this graph, the position of a molecule correlates its WLOGP and topological polar surface area (TPSA) while representing its ability to cross through biological membranes by passive diffusion. Additionally, it is shown that *BZQuin* may not be a substrate of P-glycoprotein (P-gp), an ABC transporter widely expressed in the BBB, the latter acting as an efflux pump and preventing substances from entering the CNS [28,29].

For a comprehensive in silico evaluation of the possible interactions between *BZQuin* and glutamate receptors, six different metabotropic receptors, with two from each existing group, and two isoforms of the ionotropic NMDA receptor were evaluated as possible targets. The complete results obtained from each evaluated glutamate receptor and ligand are listed in Supplementary Table S2. In these results, the endogenous ligands *L*-glutamate and *D*-aspartate bound to the *L*-glutamate sites on all of the evaluated glutamate receptors, as expected. In contrast to this, Quin, which structurally resembled *D*-aspartate, bound to the *L*-glutamate site on the synaptic and extrasynaptic NMDA receptors, with more negative Gibbs binding energy (ΔG) than *L*-glutamate and *D*-aspartate. This suggested higher affinity between Quin and the explored receptor. The results obtained for Quin are in accordance with its action as an agonist at the NMDA receptor, directly binding to its *L*-glutamate site [14]. Additionally, Quin bound to the metabotropic mGluR1, mGluR2, and mGluR3 receptors with higher affinities and higher probabilities than the two evaluated EAAs. When comparing the *BZQuin* results against those of its precursor, it becomes clear that its affinity to the *L*-glutamate sites on mGluR1, mGluR2, and mGluR7 was higher, but that it was completely lost at the same site on the synaptic and extrasynaptic NMDA receptors. In Figure 3, the binding affinities of the evaluated ligands to the *L*-glutamate sites on mGluR1, mGluR2, and mGluR7 are plotted.

It should be noted that, although Quin had a higher affinity than the EAAs for mGluR1 and mGluR2, it did not possess affinity for mGluR7. However, the addition of the diphenylborinic moiety to the original structure appeared to be beneficial for affinity, and this was especially notable for mGluR2 and mGluR7. For the former, the ΔG changed from −6.8 kcal/mol to −10.49 kcal/mol after the structural modifications leading to *BZQuin*. For the latter, there was no affinity for Quin prior to the structural modifications.

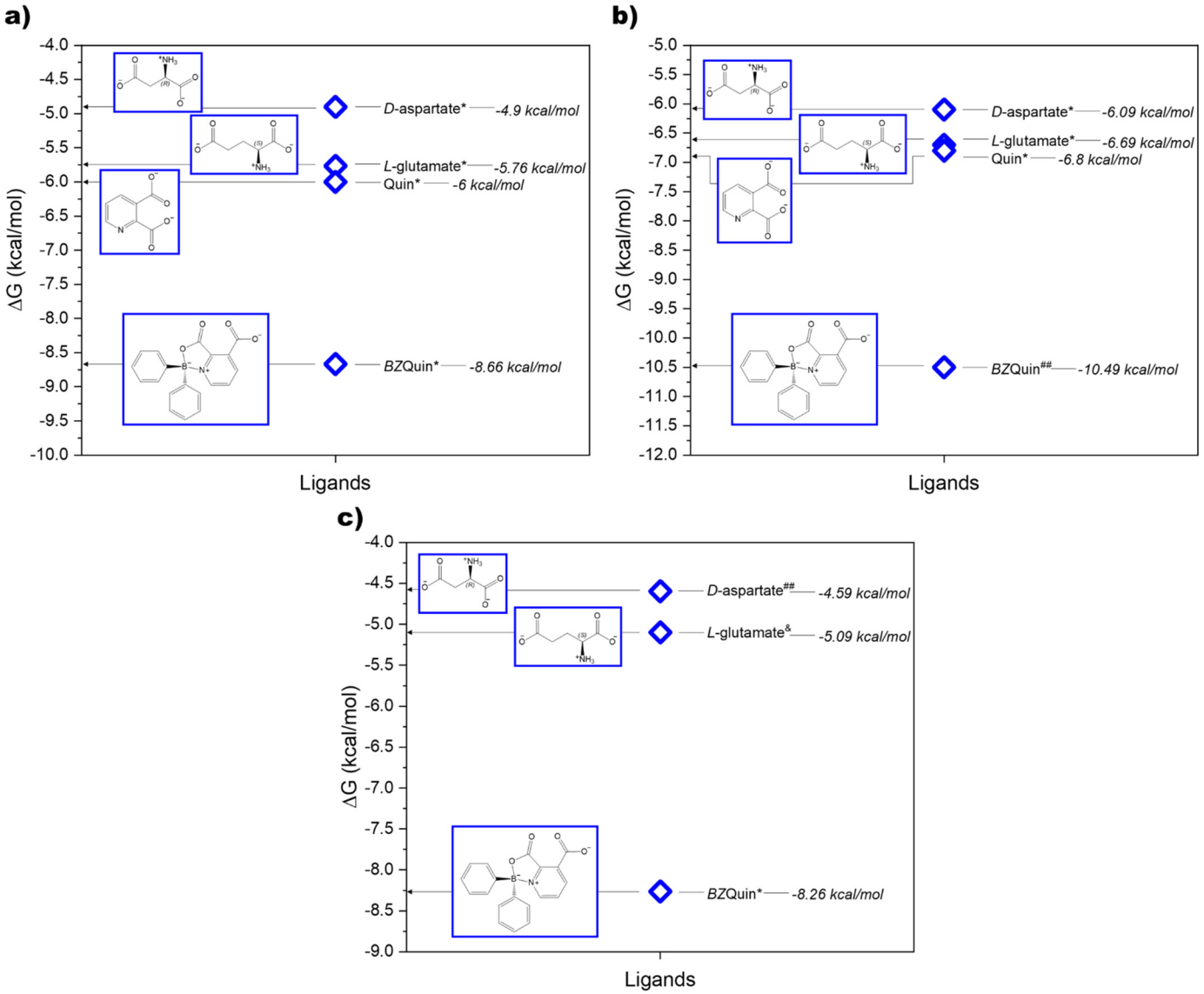

Figure 3. Ligands bound to the *L*-glutamate sites on (**a**) mGluR1, (**b**) mGluR2, and (**c**) mGluR7. Binding affinity is quantified in Δ*G*, while binding probability is represented by * $p > 0.8$, ## $p > 0.6$, & $p < 0.2$; pH = 7.4.

For the mGluR1 receptor, improvement in Δ*G* was also noticeable, but the remarkable feature is that the high binding probability ($p > 0.8$) was preserved after the structural modification. This was unlike the cases of mGluR2 and mGluR7. In Figure 4, the *BZQuin* interactions with the amino acid residues of the *L*-glutamate site on mGluR1, mGluR2, and mGluR7 are shown, along with the interactions of a cocrystallized ligand for comparative purposes. For the mGluR1 receptor, the interactions with the amino acid residues of TYR 236, SER 186, and TYR 74 were shared by the cocrystallized antagonist LY341495 and docked *BZQuin*. Thus, this suggested a possible antagonist-like behavior from *BZQuin*, which coincides with the structural resemblance between both the ligands.

However, the *in vivo* evaluation discussed later suggest the opposite. This is because the antagonism of the mGluR1 receptor contributed to neuron hyperpolarization and the absence of seizures. For the mGluR2 receptor, the interactions with amino acid residues that the cocrystallized agonist LY2812223 and docked *BZQuin* had in common were ARG 61, LYS 377, ASP 295, ALA 166, and ARG 271.

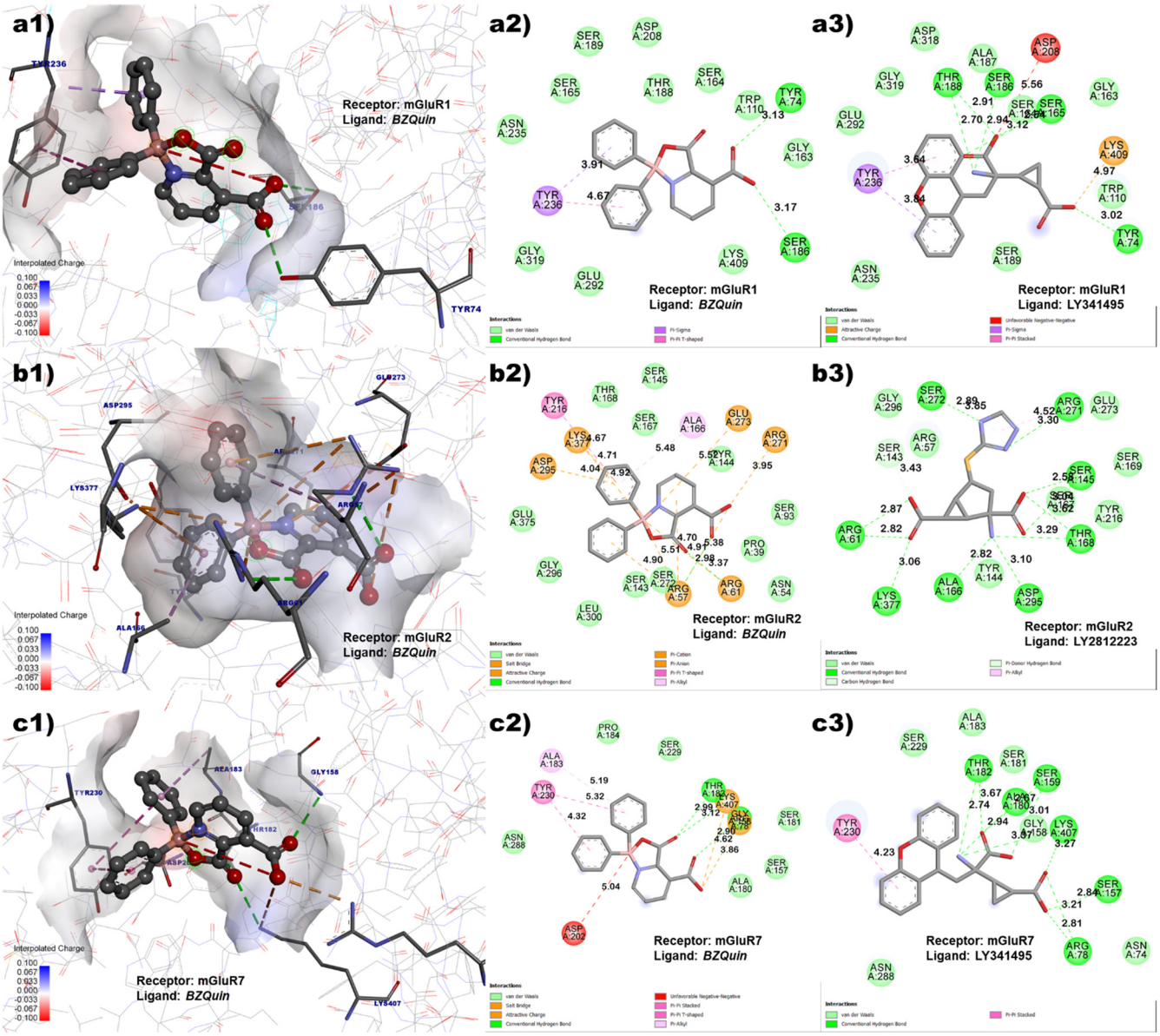

Figure 4. Pocket of the *L*-glutamate sites on (**a**) mGluR1 (PDB: 3KS9), (**b**) mGluR2 (PDB: 5CNJ), and (**c**) mGluR7 (PDB: 3MQ4). (1) Three-dimensional view of the binding mode of *BZQuin*. (2) *BZQuin* interactions with amino acid residues. (3) Cocrystallized ligand interactions with amino acid residues. Distances shown in ångströms (Å).

The number of interactions that both ligands had in common suggests that *BZQuin* could be an agonist for the mGluR2 receptor. This may not be in accordance with the in vivo results. This is due to the activation of the mGluR2 receptor that could contribute to the slow repolarization of the neuron and, hence, to the absence of seizures. Finally, for the mGluR7 receptor, the interactions with amino acid residues that the cocrystallized antagonist LY341495 and docked *BZQuin* had in common included TYR 230, THR 182, LYS 407, GLY 158, and ARG 78. The number of interactions that both ligands had in common suggests that *BZQuin* could be an antagonist for the mGluR7 receptor. This result is in agreement with the in vivo results because the antagonism of the mGluR7 receptor could result in the inability to block voltage-gated Ca^{2+} channels. This could promote *L*-glutamate exocytosis and contribute to the occurrence of low-intensity seizures [30,31].

2.2. Synthesis and Chemical Characterization

BZQuin was synthesized from the complexation of pyridine-2,3-dicarboxylic acid and diphenylborinic acid (Figure 5). The reaction was characterized by the formation of a coordinate covalent bond N→B, which occurred after the dehydration of the initial borinic ester. *BZQuin* was obtained with an 87% yield and recrystallized as clear, long, greenish prisms. To the best of the authors' knowledge, this is the first time that *BZQuin* is reported in its acid form. This is because it has only been previously isolated and characterized as an organic salt formed by the amine group from ethanolamine as a cation, with the remaining carboxylate from *BZQuin* as an anion [32]. The main evidence for the formation of *BZQuin* as an acid was the absence of the signals of the amine and methylenes from ethanolamine in the ^{1}H NMR spectrum. These would appear at 8.15 ppm for the amine and at 2.82 and 3.55 ppm for the methylenes. Additionally, the O-H$_v$ band observed in the Raman spectrum further confirmed the obtention of the acid. The successful formation of the organoboron complex was evidenced by a chemical shift of the boron atom at 9.05 ppm in the ^{11}B NMR spectrum. This signal corresponded to a tetravalent boron atom on which lay a negative charge and high electron density. This meant that its signal appeared at lower frequencies than that of a trivalent boron atom. In addition, the split observed in the multiple signal ranging from 7.36–7.12 ppm in the ^{1}H NMR spectrum corresponded to the phenyl rings bonded directly to the boron atom. This could be tentatively assigned supported by the data from the HETCOR experiment. The latter indicated that the signal splits around 7.21, 7.25, and 7.28 ppm corresponded to the hydrogen atoms in the para, meta, and ortho positions with respect to the ipso carbon, respectively. The order of these signals in the ^{1}H NMR spectrum corresponds to that from a previously reported isomer of *BZQuin*. The latter is a diphenylboroxazolidone derived from pyridine-2,6-dicarboxylic acid. The most characteristic Raman bands observed were at 2975 cm^{-1}, 1655 cm^{-1}, 1001 cm^{-1}, 955 cm^{-1}, 554 cm^{-1}, and 485 cm^{-1}. These bands corresponded to the stretching of the carboxylic acid O-H bond, borinic-ester bonds, the phenyl ring breathing mode, the stretch of the B-O bond, and two symmetric deformations in the diphenylboroxazolidone, respectively. The synthesis method presented in this article yielded 5% more product than the synthesis method reported for the salt [32,33]. In Supplementary Figures S3–S9, the *BZQuin* spectra obtained from the NMR and FT-Raman spectroscopy characterizations are shown.

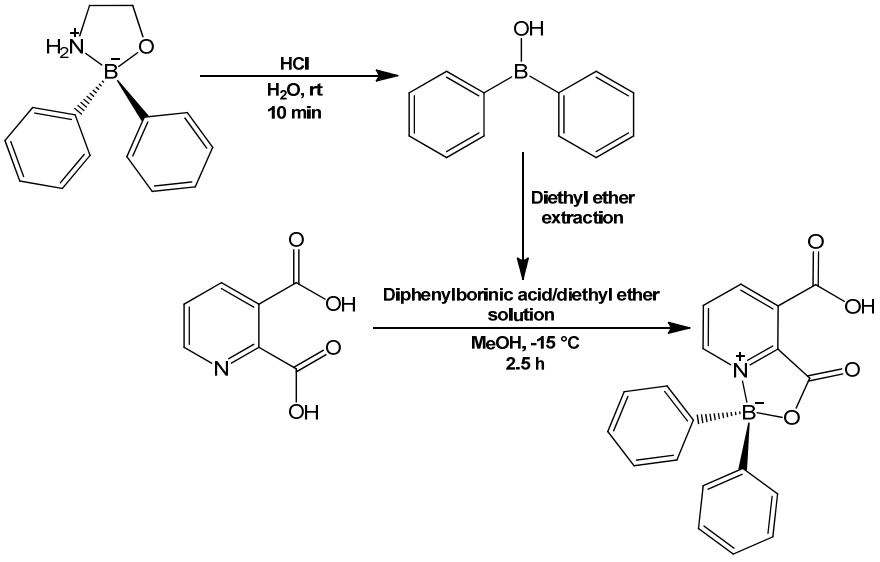

Figure 5. Synthesis of *BZQuin*. The hydrolysis of 2-APB was carried out previously and independently from the synthesis of the diphenylboroxazolidone.

Riluzole (Rlz), an antiglutamatergic drug with clinical applications that was necessary for the *in vivo* evaluation was synthesized from a one-pot synthesis reaction of 4-(trifluoromethoxy) aniline with ammonium thiocyanate and potassium persulfate as oxidizing agent (Figure 6). This was obtained with a 46% yield and recrystallized as clear yellow flakes. The main evidence of the formation of Rlz lay in the signals observed in the aromatic region of the ^{1}H NMR spectrum, which appeared at 7.37, 6.98, and 6.78 ppm and corresponded to the hydrogens in positions 7, 4, and 5, respectively. The most characteristic Raman bands observed were at 1270 cm^{-1}, 528 cm^{-1}, and 461 cm^{-1}, which corresponded to the Kekulé mode and the thiazole symmetric and antisymmetric deformations, respectively. In Supplementary Figures S10–S15, the Rlz spectra obtained from the NMR and FT-Raman spectroscopic characterizations are shown.

Figure 6. Synthesis of Rlz. The formation of its hydrochloric acid salt for purification (not shown) was carried out from a raw product using HCl and reverted using NH_4OH.

2.3. In Vivo Evaluation: Acute Toxicity

For the acute toxicity evaluation, the lethal dose 50 (LD_{50}) amount for *BZQuin* was estimated in male CD-1 mice with a modified version of Lorke's method [34]. For the complete results obtained in both phases of the experiment, see Supplementary Table S3. In Figure 7, the *BZQuin* dose–response curve is presented. This is because the observed effect, death, was of a quantal nature, the probability of which was represented in probit. Additionally, the data fitted to the linearized Hill equation are also shown. Along the *BZQuin* curves, the data for its precursor, Quin, are also plotted for comparative purposes, as derived from early reports on the toxicity of kynurenines in mice [34,35].

In the dose–response curves, the LD_{50} value was estimated by geometric mean (*G*), as described by Lorke's method [34]. It was 178 mg/kg for *BZQuin*, while it was 380 mg/kg for Quin. If the LD_{50} value was estimated with the values obtained from the data fitted to the linearized Hill equation, it could differ from that obtained by *G*. According to these, the LD_{50} value of *BZQuin* was 170 mg/kg, while for Quin, it was 309 mg/kg. Considering the LD_{50} estimations performed by both methods for each compound, it is safe to say that the LD_{50} value of *BZQuin* lay around 174 mg/kg. However, the difference between both LD_{50} values estimated for Quin left a much broader interval for a correct assessment to be carried out. Despite this, the published report from which Quin data were taken included the experimental LD_{50}, which was 360 mg/kg [35], thus narrowing the interval to around 370 mg/kg. Regardless of the LD_{50} estimations considered, it can be affirmed that *BZQuin* was around two times more toxic than Quin for male CD-1 mice when administered i.p. This was observed in the typical left-side shift in the *BZQuin* curves with respect to the Quin curves. Additionally, the difference between the slope values obtained from the linearized Hill equation fits suggested a different mechanism of action for both compounds [35,36].

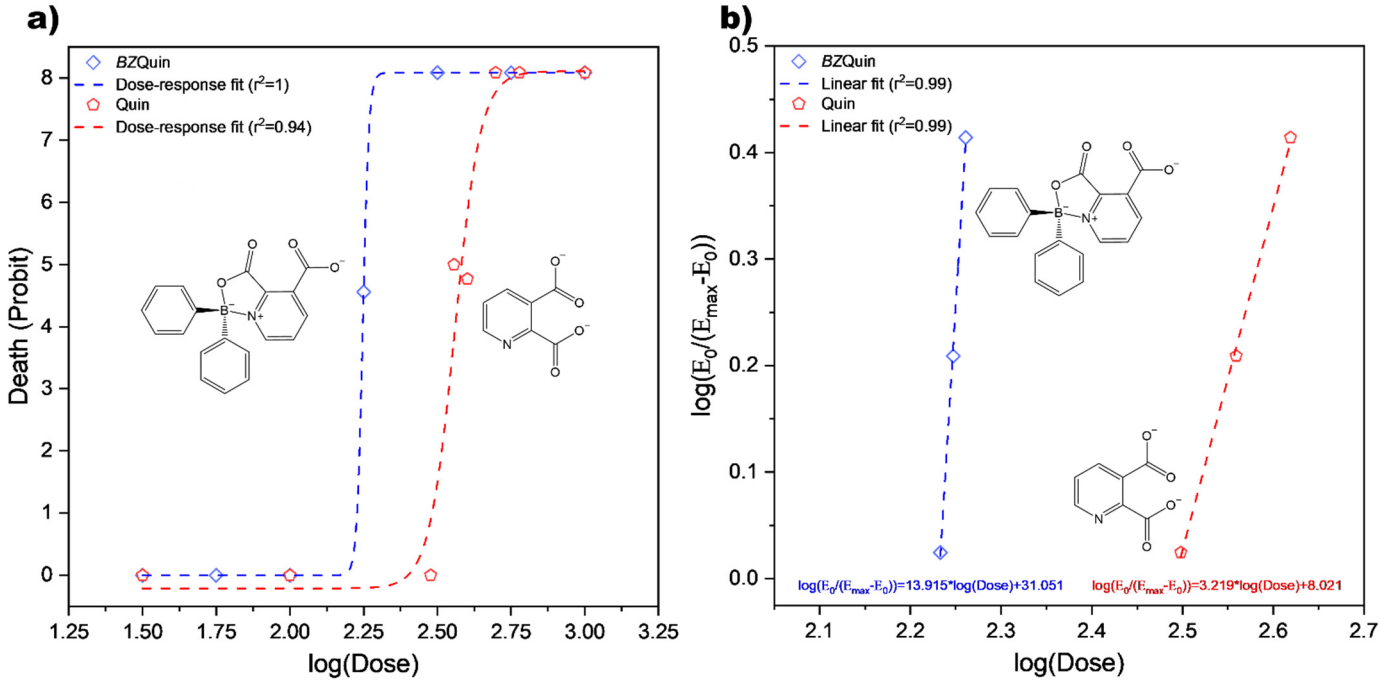

Figure 7. Acute toxicity evaluation. (**a**) *BZQuin* and Quin dose–response curves. (**b**) *BZQuin* and Quin data fitted to linearized Hill equation.

A subsequent autopsy conducted on the mice administered with *BZQuin* that did not survive revealed bleeding under the meninges. This suggests that the cause of death was due to a stroke-like event, which is usually characterized by the presence of excitotoxicity. This indicates that the effects exerted by *BZQuin* and Quin at deleterious concentrations were similar because both affected the brain directly. The autopsy carried out on the surviving mice did not reveal any macroscopic signs of pathological changes in the heart, lungs, liver, kidneys, or brain. No hematological changes were explored in this study.

2.4. In Vivo Evaluation: Murine Behavioral Model

The open field test (OFT) was applied after administrations of antiglutamatergic pretreatments and stimulating agents and the survival after these treatments. This model was designed to study the effects of *BZQuin* on behaviors often associated with the stimulation of glutamatergic neurotransmission and the possible interference of antiglutamatergic drugs with these. Quin and *BZQuin* were used as stimulating agents, with the former evaluated at 300 mg/kg and the latter at 593 mg/kg and 100 mg/kg. Memantine (Mem) and riluzole (Rlz) were used as antiglutamatergic pretreatments and were both administered at 10 mg/kg. The experimental design, drugs, and administrations are described in detail in the Materials and Methods section. The first parameter of interest in the OFT was locomotor activity, which was directly measured by the number of events. In Figure 8, the results for locomotor activity recorded over 10 min are shown. In Figure 8a, the data are plotted as boxes and whiskers since the Shapiro–Wilk normality test was failed ($p < 0.050$) while considering the vehicle group. A Kruskal–Wallis test ($H = 68.29$, $p \leq 0.001$) was conducted for comparing the vehicle group against the remainder of the groups in search of differences. In Figure 8b, for a more in-depth analysis of the relationship between the pretreatment and the stimulating agent, the vehicle group was obviated to leave the data with a normal distribution suitable for a two-way ANOVA. This graph is plotted as bars because the Shapiro–Wilk normality test was passed ($p > 0.050$).

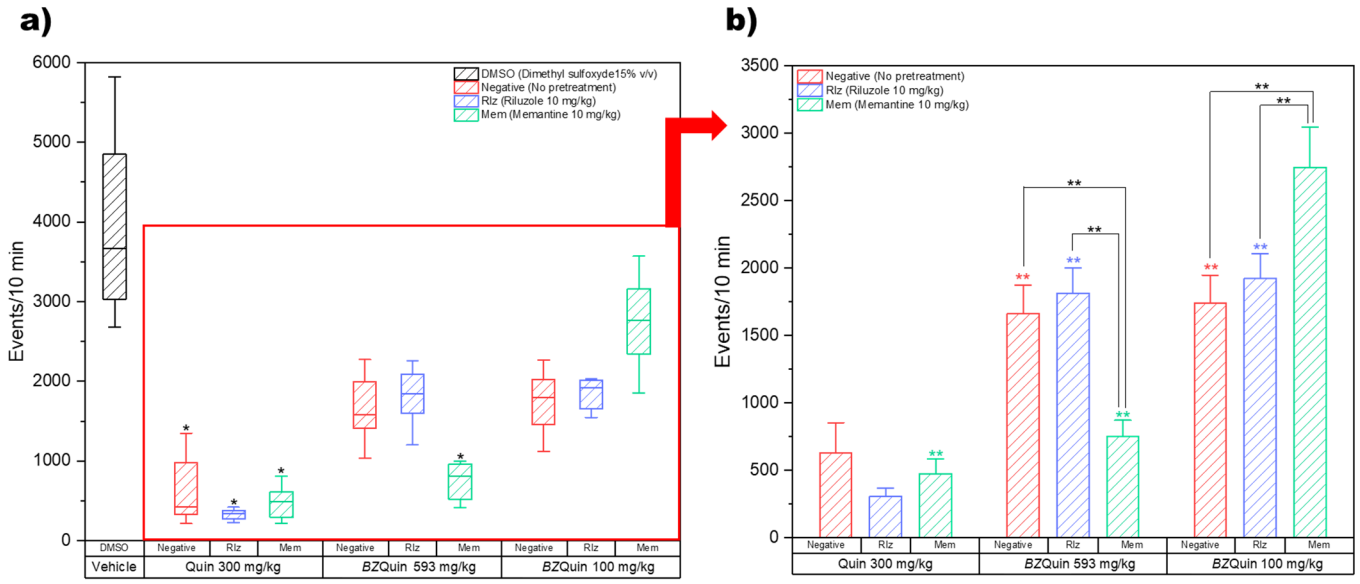

Figure 8. Locomotor activity results (events/10 min). (**a**) Non-normal distribution data considering the vehicle group. * $p < 0.05$ compared to the vehicle group. (**b**) Normal distribution data not considering the vehicle group. Events/10 min (stimulating agent): *BZQuin* 100 mg/kg > *BZQuin* 593 mg/kg > Quin 300 mg/kg, $p < 0.001$. ** $p < 0.01$. ** $p < 0.01$ compared to the negative group with Quin 300 mg/kg. ** $p < 0.01$ compared to the Rlz group with Quin 300 mg/kg. ** $p < 0.01$ compared to the Mem group with *BZQuin* 100 mg/kg.

For the interpretation of the locomotor activity results, it should be noted that a decrease in the number of events may be related to the onset and occurrence of seizures. As the intensity of the seizures increased, the locomotor activity, in turn, decreased. It is noteworthy that the locomotor activity was significantly decreased in all the groups administered with Quin at 300 mg/kg as a stimulating agent ($p < 0.05$) (Figure 8a). This indicated more intense seizures in these groups. This is in agreement with Quin as an NMDA receptor agonist. As such, it directly promoted neuron depolarization and action potential firing, which in turn gave rise to the occurrence of seizures [14]. The two-way ANOVA indicated that the results were mostly influenced by the stimulating agent administered rather than by the pretreatment (Figure 8b). In a global comparison of the factors, the least square means (LSM) of the pretreatments indicate that there was no significant difference between any of these. In contrast to this, the LSM of the stimulating agents indicate that the locomotor activity was significantly decreased in the following order: *BZQuin* at 100 mg/kg; *BZQuin* at 593 mg/kg; and Quin at 300 mg/kg ($F = 88.70$, $p < 0.001$). This indicates that the ability of *BZQuin* for causing seizures was decreased when compared with its precursor, even when administered at an equimolar dose. For the LSM and their standard errors of the mean (SEMs) for the pretreatments and the stimulating agents, see Supplementary Table S4. Additionally, in a simple comparison of the LSM of each interaction, there existed significant differences among the groups with the same pretreatment but administered with a different stimulating agent ($F = 14.42$, $p < 0.001$). The locomotor activity of the group with no pretreatment (negative) administered with Quin at 300 mg/kg was significantly decreased when compared with the negative groups administered with *BZQuin* at 593 mg/kg and at 100 mg/kg ($p < 0.01$). A similar situation was observed with the group pretreated with Rlz at 10 mg/kg and administered with Quin at 300 mg/kg. This was due to its locomotor activity being significantly decreased when compared with the Rlz groups administered with *BZQuin* at 593 mg/kg and 100 mg/kg ($p < 0.01$). In contrast to this, the locomotor activity of the group pre-treated with memantine (Mem) at 10 mg/kg and administered with *BZQuin* at 100 mg/kg was significantly increased when compared with the other two Mem groups ($p < 0.01$). An interesting observation is that, when *BZQuin* was administered at 593 mg/kg, Mem appeared to contribute to the decrease in locomotor

activity. Nonetheless, when *BZQuin* was administered at 100 mg/kg, Mem significantly increased it. For the LSM and SEMs for the interaction, see Supplementary Table S5. Both types of comparisons performed indicate that, regardless of the pretreatment or the dose of *BZQuin* administered, Quin decreased locomotor activity to a greater extent than its organoboron derivative.

Although Rlz-pretreated groups had no significant differences in locomotor activity when compared with the negative groups, Mem behaved differently depending on the *BZQuin* dose administered. The effects of these drugs were more noteworthy during the latency time until the occurrence of seizures and their intensity. In Table 1, the results for the latency time are presented. Each mouse was observed for 15 min prior to the start of the OFT. Because the latency time of the groups administered with *BZQuin* at 593 mg/kg and 100 mg/kg surpassed the observation time, they were not considered for the statistical analysis. On the other hand, the latency times of the groups administered with Quin at 300 mg/kg passed the Shapiro–Wilk normality test ($p < 0.050$); therefore, they were compared with a one-way ANOVA.

Table 1. Latency time until the occurrence of the first Racine stage of immobility. The latency time was accounted for during the first 15 min after the administration of the stimulating agent and corresponded to the arithmetic means and SEMs of each group.

Group		Latency Time (min)
Pretreatment	**Stimulating Agent**	
Negative (no pretreatment)	Quin at 300 mg/kg	5.49 ± 0.62
Rlz (riluzole 10 mg/kg)		* 8.13 ± 0.30
Mem (memantine 10 mg/kg)		6.61 ± 0.36
Negative (no pretreatment)	*BZQuin* at 593 mg/kg	<15
Rlz (riluzole 10 mg/kg)		<15
Mem (memantine 10 mg/kg)		<15
Negative (no pretreatment)	*BZQuin* at 100 mg/kg	<15
Rlz (riluzole 10 mg/kg)		N/A
Mem (memantine 10 mg/kg)		N/A

* Longer latency time when compared with the negative group of Quin at 300 mg/kg, $p < 0.01$. N/A = not applicable.

The latency time results indicate that the only significant difference was among the groups administered with Quin at 300 mg/kg, specifically, between the Rlz and negative groups. The longer latency time of the Rlz-pretreated group was related to the delay in the onset of seizures. The latter may be attributed to the antiglutamatergic effect that this pretreatment drug exerted and its interference with the glutamatergic mechanism of Quin. After the initial 15 min of observation, the intensity of the seizures was evaluated according to Racine stages, which are employed when a glutamatergic agent is administered to induce status epilepticus [37] (Figure 9).

The data are plotted as boxes and whiskers because the Shapiro–Wilk normality test was failed ($p < 0.050$). Because the data could not be analyzed by parametric tests, three Kruskal–Wallis tests were carried out. The first of these was for comparing the effect of the pretreatments ($H = 22.19$, $p \leq 0.001$). The second was carried out to compare the effect of the stimulating agents ($H = 32.06$, $p \leq 0.001$), while the third was to compare each individual group against the others ($H = 62.09$, $p \leq 0.001$). For the medians (P_{50}) and percentiles (P_{25} and P_{75}) of the pretreatments and stimulating agents, see Supplementary Table S6.

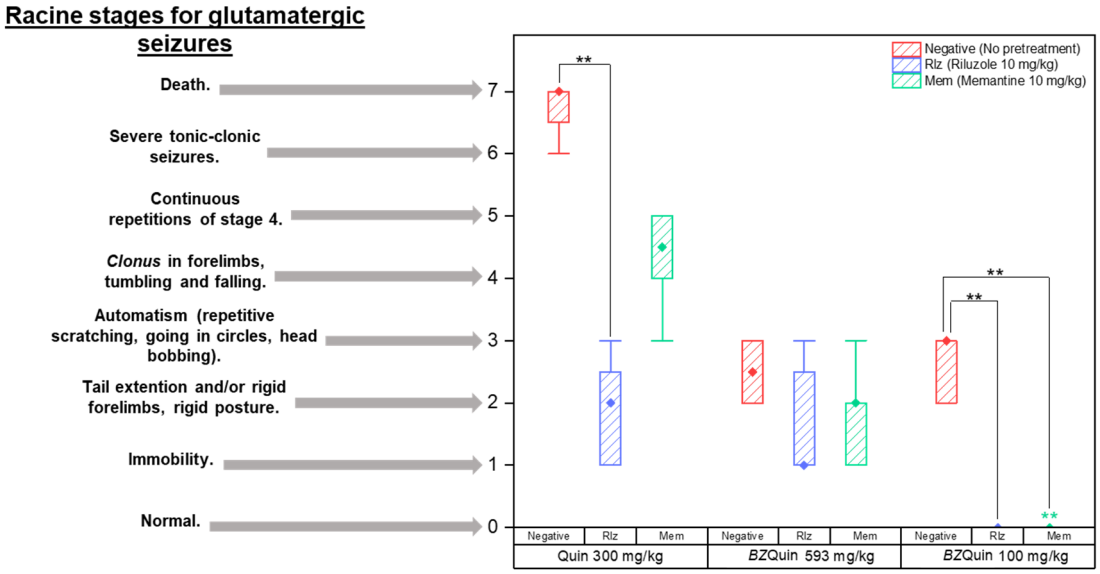

Figure 9. Classification of the intensity of seizures (Racine stages). Non-normal distribution data not considering the vehicle group. Racine stage (pretreatment): negative > Rlz = Mem, $p < 0.001$. Racine stage (Stimulating agent): Quin 300 mg/kg > *BZQuin* 593 mg/kg > *BZQuin* 100 mg/kg, $p < 0.001$. ** $p < 0.001$. ** $p < 0.001$ compared with the Mem group with Quin at 300 mg/kg.

For comparison of the pretreatments, it was observed that the intensity of the seizures increased in the negative groups as expected due to the lack of pretreatment with an antiglutamatergic drug. Notwithstanding this, there was no difference between the groups pretreated with Rlz or Mem ($p < 0.001$). Considering these results, it should be noted that both antiglutamatergic drugs interfered with the effects of both stimulating agents, with the latter reflected in the low-intensity seizures observed in the Rlz and Mem groups. For *BZQuin*, an unexplored compound, this suggested that its effects may be related to glutamatergic neurotransmission. For comparison of the stimulating agents, it was observed that the intensity of the seizures increased in the following order: *BZQuin* at 100 mg/kg; *BZQuin* at 593 mg/kg; and Quin at 300 mg/kg ($p < 0.001$). The fact that *BZQuin*, even at an equimolar dose compared to Quin, was no longer capable of inducing high-intensity seizures strongly suggested that it does not interact with the NMDA receptor. These *in vivo* results correlate with the *in silico* results from the previously discussed molecular docking. Additionally, along with the locomotor activity results, these suggested once again that mGluRs may be the targets for *BZQuin* due to the excitatory glutamate-related slow response observed in the administered groups. For the individual-group comparison, among the groups administered with Quin at 300 mg/kg, it was observed that the intensity of seizures was significantly decreased in the group pretreated with Rlz when compared with the negative group ($p < 0.001$). Meanwhile, among the groups administered with *BZQuin* at 100 mg/kg, it was observed that seizure intensity was significantly decreased in the groups pretreated with Rlz and Mem when compared with the negative group ($p < 0.001$). These results indicate more clearly that the effects of *BZQuin* were related, at least partially, to its positive influence on glutamatergic neurotransmission. This can be affirmed due to the interference exerted by both antiglutamatergic drugs with its effects. Additionally, in the group pretreated with Mem, there was a significant decrease in seizure intensity when compared with its homologue administered with Quin at 300 mg/kg as a stimulating agent ($p < 0.001$). After the OFT, the mice of each group were observed for 15 days to evaluate survival. In Supplementary Figure S2, survival amounts of the mice at 48 h and at 15 days are represented as bars.

It was observed from the survival at 48 h that, between the groups administered with equimolar doses of *BZQuin* and Quin, none of the mice from the former groups survived after 48 h, regardless of the pretreatment administered. Among the groups administered

with Quin at 300 mg/kg, after 48 h, all mice pretreated with Rlz survived, while three of the mice pretreated with Mem and the majority of the mice from the negative group died. These results demonstrate that, in addition to the already-observed antiglutamatergic effect of Rlz, this drug also improved survival when used against Quin, performing even better than Mem. Among the groups administered with *BZQuin* at 100 mg/kg, after 48 h, the majority of the mice survived, except for one mouse pretreated with Mem. Therefore, this indicated that perhaps, at a dose below 100 mg/kg, *BZQuin* may have possible biological applications without toxic effects. From the survival at 15 days, among the groups administered with Quin at 300 mg/kg, the majority of the mice pretreated with Mem died compared with one mouse pretreated with Rlz. This implied that Mem may not be as good as Rlz for improving survival after an acute excitotoxic event. The fact that, at the end of the experiment, the negative group had a survival probability of 0.25 was not in accordance with its estimated and reported LD_{50}. However, *BZQuin* at an equimolar dose compared with that of Quin remained toxic. Among the groups administered with *BZQuin* at 100 mg/kg, after 15 days, two of the mice from the negative group died, while all mice pretreated with Rlz and the rest of the mice pretreated with Mem survived. This suggests that Rlz and Mem exerted an effect on the survival of these groups by antagonizing the effects of *BZQuin*. This is in agreement with Rlz and Mem preventing at all times the occurrence of seizures among the mice of these groups.

2.5. Ex Vivo Evaluation: Nervous Tissue Histology

The ex vivo evaluation was carried out on the mice in groups not treated (normal), administered with vehicle, and the surviving groups, which were those administered with Quin at 300 mg/kg and with *BZQuin* at 100 mg/kg. This was performed to observe the effects of the pretreatments and the stimulating agents on neuronal survival using the method of Vogt for neuron staining on brain sections. The neuroanatomical structures of interest in which the neurons were accounted for included the ventral hippocampus, the striatum, and the prefrontal and cerebellum cortexes. A decrease in neuron count was related to neurotoxicity. Therefore, due to the consideration that the stimulating agents Quin and *BZQuin* exerted a positive influence on glutamatergic neurotransmission, the observed neurotoxicity could be considered a manifestation of excitotoxicity. Micrographs of the regions of the four studied neuroanatomical structures at magnifications of 4× and 20× are presented in this section for demonstrative purposes.

In Figure 10, the results for the neuron count in the CA1 region of the ventral hippocampus and the striatum are shown. In these graphs, the data are plotted as bars since, for both, the Shapiro–Wilk normality test was passed ($p > 0.050$). For the ventral hippocampus, a one-way ANOVA indicated that the neuron count was significantly decreased in the majority of the groups. Among the groups administered with Quin at 300 mg/kg, the only group with no significant difference against the normal and vehicle groups was that pretreated with Rlz. This indicates that the neuroprotective effect of Rlz was particularly good at the CA1 region of the ventral hippocampus. Among the groups administered with *BZQuin* at 100 mg/kg, the three groups showed a significant decrease in neuron count when compared to the normal group ($p < 0.05$). However, only the group pretreated with Mem demonstrated a significant decrease in neuron count when compared to the vehicle group ($p < 0.01$). A global comparison of the LSM of the pretreatments in a two-way ANOVA revealed that the neuron count was significantly decreased in the following order: Rlz, Mem, and negative ($F = 23.68$, $p < 0.001$). Thus, this indicates that Rlz possessed a better neuroprotective effect that Mem in the analyzed region but that both improved neuronal survival. In addition to this, when performing the global comparison for the stimulating agents, the neuron count was significantly lower in the groups administered with Quin at 300 mg/kg than in the groups administered with *BZQuin* at 100 mg/kg ($F = 25.38$, $p < 0.001$). This implies that *BZQuin* was not as toxic as Quin for the neurons of the analyzed region. This is coherent with the fact that the negative group administered with *BZQuin* at 100 mg/kg entertained no difference from the vehicle group.

In a simple comparison of the LSM of the interactions, there existed a significant difference between some of the groups (F = 21.33, $p < 0.001$). Among the groups administered with Quin at 300 mg/kg, on comparing the group pretreated with Rlz against the negative and Mem groups, there was a decrease in the neuron count of the latter ($p < 0.001$). In the negative group, there was a significant decrease in neuron count when compared against the group pretreated with Mem ($p < 0.01$). This is in agreement with the global comparison of the pretreatments because the neuron count decreased significantly in the same order. The most relevant observation in the CA1 region of the ventral hippocampus is that the neuron counts of the groups administered with *BZQuin* at 100 mg/kg did not exhibit any significant difference when compared to that of the vehicle group, whether or not the mice were pretreated with Rlz. This could be related to the low expressions of mGluR1, mGluR2, and mGluR7 in this specific region of the hippocampal circuit. These results are coherent and further support the results of the molecular docking and the murine behavioral model, suggesting that *BZQuin* may exert its effects by binding to one of these mGluRs [4,38].

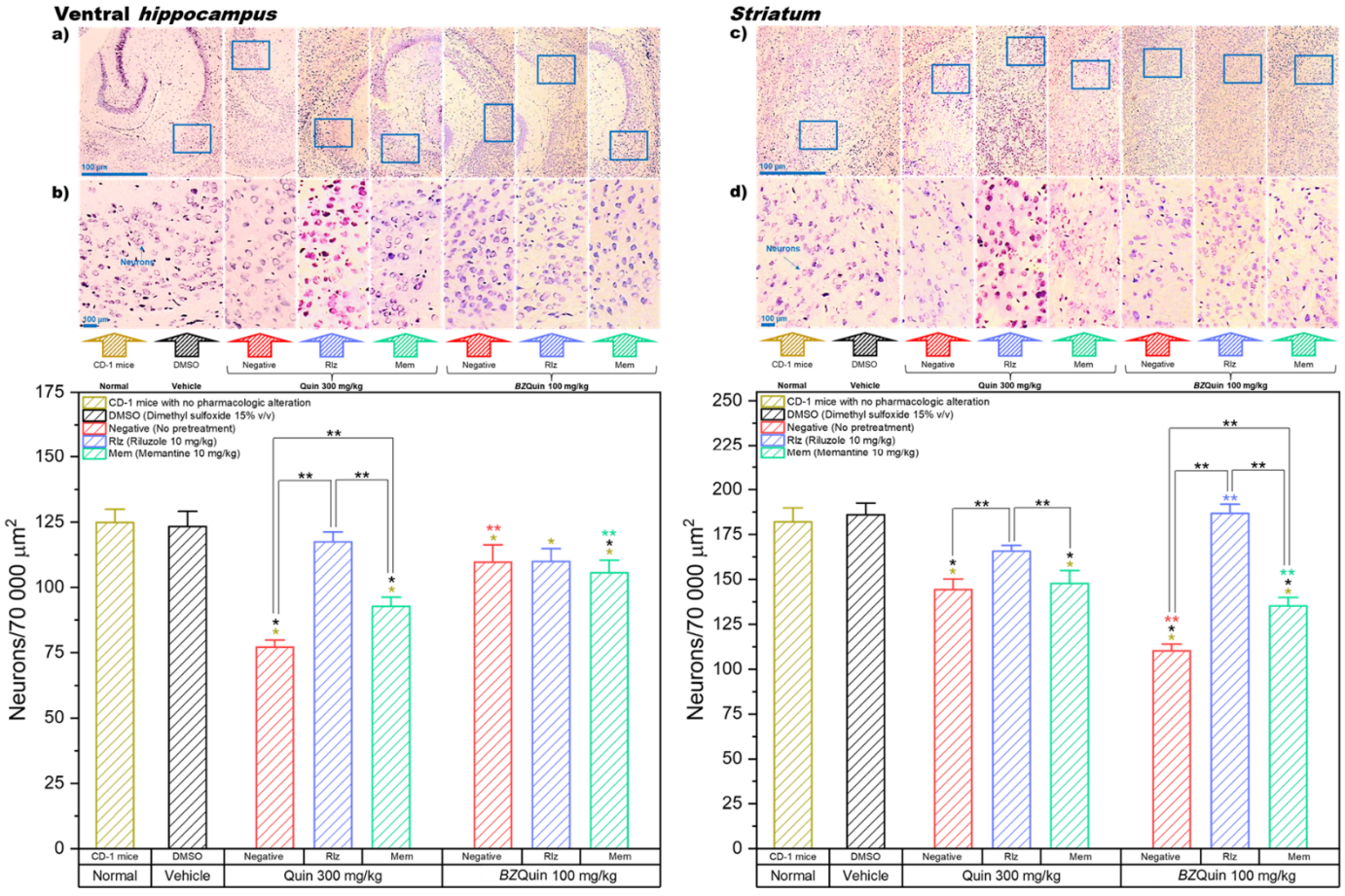

Figure 10. Left. Ventral hippocampus (neuron count in the CA1 region): * $p < 0.001$ compared to the normal group; * $p < 0.001$ compared to the vehicle group. Neurons/70,000 µm² (pretreatment): Rlz > Mem > negative, $p < 0.001$. Neurons/70,000 µm² (stimulating agent): *BZQuin* 100 mg/kg > Quin 300 mg/kg, $p < 0.001$. ** $p < 0.01$. ** $p < 0.001$ compared to the negative group with Quin at 300 mg/kg. ** $p < 0.01$ compared to the Mem group with Quin 300 at mg/kg. Micrographs at magnifications of (**a**) 4× and (**b**) 20×. **Right.** Striatum (neuron count): * $p < 0.001$ compared to the normal group; * $p < 0.001$ compared to the vehicle group. Neurons/70,000 µm² (pretreatment): Rlz > Mem > negative, $p < 0.001$. Neurons/70,000 µm² (stimulating agent): Quin 300 mg/kg > *BZQuin* 100 mg/kg, * $p < 0.01$. ** $p < 0.01$. ** $p < 0.001$ compared to the negative group with Quin at 300 mg/kg. ** $p < 0.001$ compared to the Rlz group with Quin at 300 mg/kg. ** $p < 0.05$ compared to the Mem group with Quin at 300 mg/kg. Micrographs at magnifications of (**c**) 4× and (**d**) 20×.

For the striatum, a one-way ANOVA indicated that the neuron count was significantly decreased in the majority of the groups. Among the groups administered with Quin at 300 mg/kg and among those administered with *BZQuin* at 100 mg/kg, the negative and Mem groups revealed a significant decrease in neuron count when compared to the normal and vehicle groups ($p < 0.001$). In both groups pretreated with Rlz, this drug exerted a neuroprotective effect, regardless of the stimulating agent administered. Therefore, there were no significant differences from the normal and vehicle groups. A global comparison of the LSM of the pretreatments in a two-way ANOVA demonstrated that the neuron count was significantly decreased in the following order: Rlz, Mem, and negative ($F = 103.67$, $p < 0.001$). Additionally, upon conducting a global comparison for the stimulating agents, the neuron count was significantly lower in the groups administered with *BZQuin* at 100 mg/kg than in the groups administered with Quin at 300 mg/kg ($F = 8.86$, $p < 0.01$). These global comparisons indicate that the neuroprotective effect of Rlz outperformed that of Mem in the striatum, while *BZQuin* appeared to exert a greater neurotoxic effect than Quin in this same region, even at a lower molar dose. This could be attributed to an excitatory effect on neurons and a higher affinity for glutamate receptors. In a simple comparison of the LSM of the interactions, there existed a significant difference between some of the groups ($F = 32.21$, $p < 0.001$). Among the groups administered with Quin at 300 mg/kg, the group pretreated with Rlz revealed a significant decrease in neuron count when compared against the negative and Mem groups ($p < 0.01$). A similar situation was observed for the groups administered with *BZQuin* at 100 mg/kg ($p < 0.001$). However, the neuron count in the group pretreated with Mem was even higher than that of the negative group ($p < 0.001$). This demonstrated the neuroprotective effect of Mem against *BZQuin*, although it was not as good as Rlz. Finally, when comparing both negative groups, the neuron count of the group administered with *BZQuin* was lower than that of the group administered with Quin ($p < 0.001$). This is in agreement with the global comparisons and further implies the possible selectivity of *BZQuin* for the neurons in the striatum. This same observation could be made when comparing both groups pretreated with Mem. The group administered with *BZQuin* had the lowest neuron count ($p < 0.001$). However, an inverse situation was observed among the groups pretreated with Rlz, in which the neuron count of the group administered with *BZQuin* was the highest ($p < 0.001$). This demonstrated the neuroprotective effect of Rlz against *BZQuin* in the striatum. With these results, it could be affirmed that *BZQuin* exerts a greater influence on the neuron count in the striatum than its precursor, while the antiglutamatergic drugs Rlz and Mem interfered with its effects. A possible explanation behind the *BZQuin* effect could be the high expressions of iGluRs in the dopaminergic and glutamatergic neurons in the striatum. The latter is especially remarkable for the thalamo-striatal pathway, in which the mGluR1 receptor is highly expressed. These results are complementary to the molecular-docking results. These results propose the mGluR1 receptor as one of the possible targets for *BZQuin*, with its binding site located at the *L*-glutamate site. The fact that *BZQuin* exerted a neurotoxic effect that was countered by antiglutamatergic drugs strongly suggests a positive influence on glutamatergic neurotransmission [4,39].

In Figure 11, the results are presented for the neuron counts in the prefrontal and cerebellum cortexes of the brain. In these graphs, the data are plotted as bars because, for both, the Shapiro–Wilk normality test was passed ($p > 0.050$). For the prefrontal cortex, a one-way ANOVA indicated that the negative and Mem groups administered with Quin at 300 mg/kg as a stimulating agent, as well as all the groups administered with *BZQuin* at 100 mg/kg, demonstrated a significant decrease in neuron count when compared to the normal and vehicle groups ($p < 0.001$). The neuroprotective effect of Rlz was better observed in the prefrontal cortex when it was administered as a pretreatment against Quin, in that there was no significant difference from the normal and vehicle groups. A global comparison of the LSM of the pretreatments in a two-way ANOVA revealed that the neuron count was significantly decreased in the following order: Rlz, negative, and Mem ($F = 89.25$, $p < 0.001$). It is important to highlight that, in the prefrontal cortex, Rlz once again

exerted a remarkable neuroprotective effect, although only when used as a pretreatment against Quin. Additionally, Mem appeared to exert a synergistic neurotoxic effect when employed as a pretreatment against *BZQuin*. In addition to this, when carrying out a global comparison of the LSM of the stimulating agents, the neuron count in the groups administered with *BZQuin* at 100 mg/kg was significantly lower when compared to the neuron count in the groups administered with Quin at 300 mg/kg ($F = 59.79$, $p < 0.001$). In a simple comparison of the LSM of the interactions, there existed a significant difference between some of the groups ($F = 49.37$, $p < 0.001$).

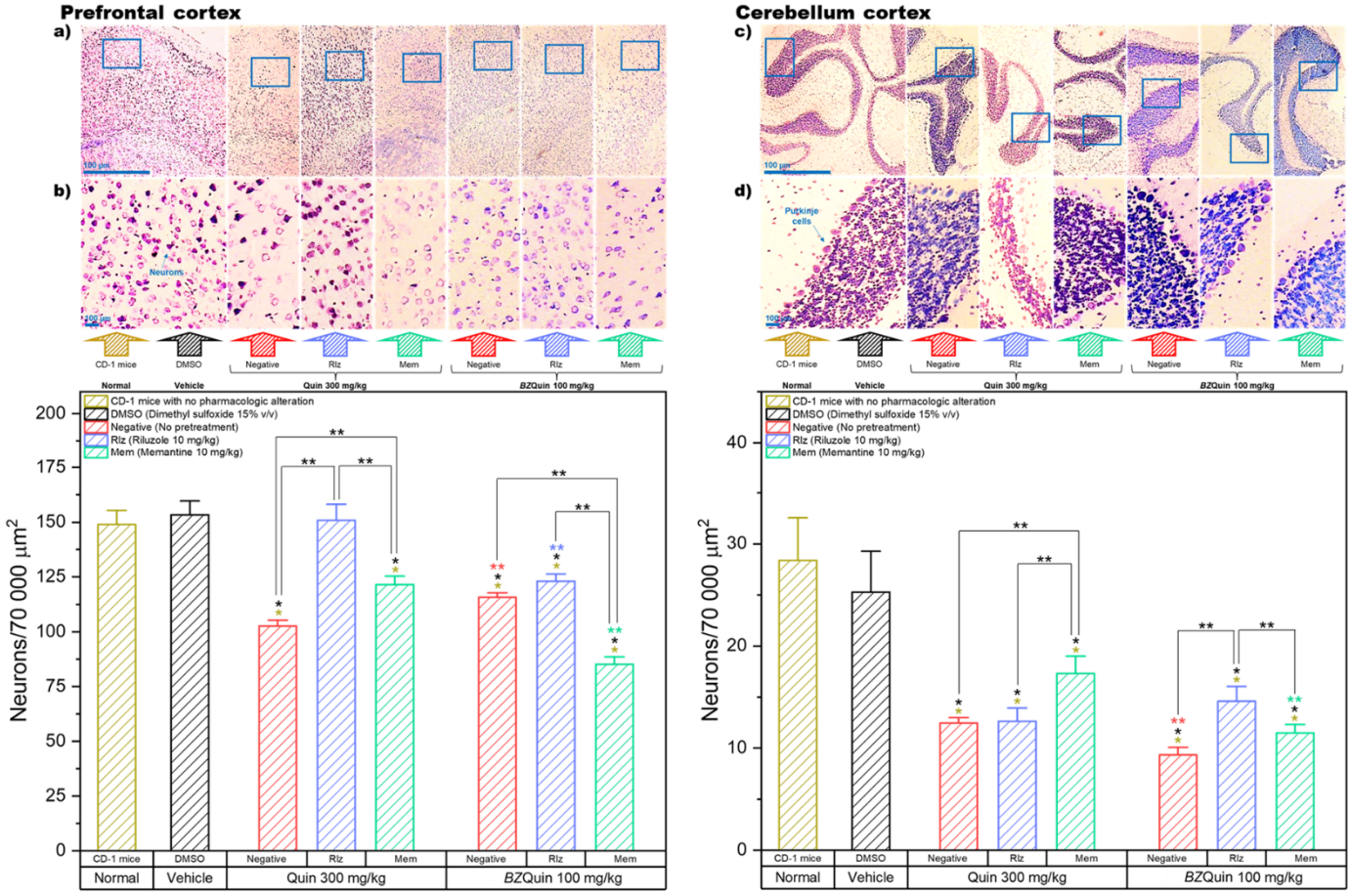

Figure 11. Left. Prefrontal cortex (neuron count): * $p < 0.001$ compared to the normal group; * $p < 0.001$ compared to the vehicle group. Neurons/70,000 µm² (pretreatment): Rlz > Negative > Mem, $p < 0.001$. Neurons/70,000 µm² (stimulating agent) : Quin 300 mg/kg > *BZQuin* 100 mg/kg, $p < 0.001$. ** $p < 0.001$. ** $p < 0.01$ compared to the negative group with Quin at 300 mg/kg. ** $p < 0.001$ compared to the Rlz group with Quin at 300 mg/kg. ** $p < 0.001$ compared to the Mem group with Quin at 300 mg/kg. Micrographs at magnifications of (**a**) 4× and (**b**) 20×. **Right.** Cerebellum cortex (neuron count, specifically Purkinje cells): * $p < 0.001$ compared to the normal group; * $p < 0.05$ compared to the vehicle group. Neurons/70,000 µm² (pretreatment): Mem > Rlz > negative, $p < 0.001$. Neurons/70,000 µm² (stimulating agent) : Quin 300 mg/kg > *BZQuin* 100 mg/kg, $p < 0.001$. ** $p < 0.05$. ** $p < 0.01$ compared to the negative group with Quin at 300 mg/kg. ** $p < 0.001$ compared to the Mem group with Quin at 300 mg/kg. Micrographs at magnifications of (**c**) 4× and (**d**) 20×.

Among the groups administered with Quin at 300 mg/kg, in the negative and Mem groups there was a significant decrease in neuron count when compared to the group pretreated with Rlz ($p < 0.001$). Another significant decrease in neuron count was observed in the negative group when compared to that pretreated with Mem ($p < 0.001$). Thus, the latter demonstrated the neuroprotective effects exerted by Rlz and Mem against Quin in the prefrontal cortex. In contrast to this, among the groups administered with *BZQuin* at

100 mg/kg, when comparing the group pretreated with Mem against the negative and Rlz groups, there was a significant decrease in the neuron count of the former ($p < 0.001$). This is in agreement with the global comparisons and further supports the observation on the synergic neurotoxicity exerted by the concomitant administration of *BZQuin* and Mem.

One of the most important differences observed was between both negative groups because the group administered with *BZQuin* at 100 mg/kg had a slightly higher, but significant, neuron count than that administered with Quin at 300 mg/kg ($p < 0.01$). An inverse situation was observed when comparing both Rlz groups against each other and both Mem groups against each other. This is because the neuron count was higher in the groups administered with Quin at 300 mg/kg ($p < 0.001$). Although Rlz and Mem were proved to exert a neuroprotective effect against *BZQuin* in the striatum, they appeared to be useless against the *BZQuin*-induced neurotoxicity in the prefrontal cortex. The ineffectiveness of these drugs against *BZQuin* could be attributed to high expressions of the mGluR1 and mGluR2 receptors in this region, both suggested targets for *BZQuin*. In addition, a high intrinsic activity of the evaluated compound with these mGluRs or its direct binding to other unexplored targets, which might not be necessarily glutamatergic, could also contribute to the observed effects [4,40].

For the cerebellum cortex, the neuron count was performed for Purkinje cells, a unique type of neuron found specifically in this part of the CNS. A one-way ANOVA indicated that, among the groups administered with Quin at 300 mg/kg and those administered with *BZQuin* at 100 mg/kg, all the groups showed a significant decrease in neuron count when compared to the normal and vehicle groups ($p < 0.001$). Thus, this indicates that neither Rlz nor Mem were sufficiently effective at protecting the Purkinje cells from the neurotoxicity induced by Quin or *BZQuin*. A global comparison of the LSM of the pretreatments in a two-way ANOVA revealed that the Purkinje cell count was significantly decreased in the following order: Mem, Rlz, and negative ($F = 11.29$, $p < 0.001$). Considering these results, the cerebellum cortex was the only studied region in which Mem exerted a better neuroprotective effect than Rlz, at least when used against Quin. In addition, when carrying out the global comparison of the LSM of the stimulating agents, it was observed that the Purkinje cell count was lower in the groups administered with *BZQuin* at 100 mg/kg than in the groups administered with Quin at 300 mg/kg ($F = 13.21$, $p < 0.001$). Thus, this suggested that *BZQuin* may exert greater effect on Purkinje cell count than Quin. This could be interpreted as an improved selectivity for the neurons of this area similar to what was observed in the striatum. In a simple comparison of the LSM of the interactions, there existed a significant difference among the groups ($F = 12.93$, $p < 0.001$). Among the groups administered with Quin at 300 mg/kg, upon comparison of the negative and Rlz groups to the Mem group, the Purkinje cell count of the latter was significantly higher ($p < 0.001$). This confirms the ineffectiveness of Rlz against Quin in this area and the better neuroprotective effect exerted by Mem. Among the groups administered with *BZQuin* at 100 mg/kg, upon comparing the group pretreated with Rlz against the negative and Mem groups, there was a significant decrease in the Purkinje cell counts of the latter ($p < 0.05$). This demonstrates that Rlz exerted a neuroprotective effect on the Purkinje cells against *BZQuin*, while Mem was ineffective against this stimulating agent. These statements are further supported by the comparisons between both Mem groups and both negative groups. In these, the groups administered with *BZQuin* exhibited a significant decrease in the Purkinje cell count when compared to their homologues administered with Quin ($p < 0.01$). The fact that *BZQuin* exerted a greater neurotoxic effect on Purkinje cells could be attributed to the mGluR that this unique type of neuron expresses. This is because they only express the mGluR1 and mGluR7 receptors, which were both suggested as targets for *BZQuin* by molecular docking. In addition, Quin was suggested to be unable to bind to the mGluR7 receptor by the same molecular-docking results [4,41,42].

3. Materials and Methods

3.1. In Silico Evaluation: ADME Properties and Molecular Docking on Glutamate Receptors

The SwissADME server from the Swiss Institute of Bioinformatics (http://www.swissadme.ch/ accessed 5 June 2022 [28]) was used to predict the pharmacokinetic and physicochemical properties of *BZQuin*. From the information that SwissADME can provide, pharmacokinetic data such as GI absorption, BBB permeability, and the possibilities of being a P-gp substrate or a CYP inhibitor were obtained for *BZQuin*, for its precursor (Quin), and for the *L*-glutamate and *D*-aspartate endogenous neurotransmitters. Additionally, the predicted values were also obtained for the physicochemical properties considered by the Lipinski Rule of Five for a good possible drug, as well as those needed for building a BOILED-Egg graph, which represents passage through biological membranes by means of passive diffusion [28,29].

The ligands utilized for molecular docking included the endogenous ligands *L*-glutamate, *D*-aspartate, and Quin, which were included as references. These structures, along with *BZQuin*, were drawn in 2D in ChemSketch, considering the predominant microspecies at a pH of 7.4, and were later transformed into their 3D models. Then, these 3D structures were geometrically optimized to the lowest-energy conformer in Gaussian 16W employing the semi-empirical method of Austin Model 1 (AM1). The Gasteiger charges and torsion restriction for the rotatable bonds in each ligand were added with AutoDock Tools version 1.5.6. For *BZQuin*, which contained a tetravalent boron atom, it was replaced with a carbon atom in the .pdbqt file, as required by the docking program. The structures of the glutamate receptors were retrieved from the Protein Data Bank and were prepared for molecular docking using Discovery Studio 2019, where the water molecules and cocrystallized ligands were removed. The Kollman charges and the polar hydrogens of each protein were added with AutoDock Tools version 1.5.6. With this same software, the search space size (100 $Å^3$) and coordinates were defined, as well. The software employed for performing the simulations was AutoDock Vina version 1.1.2. Each of these was performed along 1000 repetitions. The data obtained from these in silico experiments included the binding probability, the binding affinity quantified in ΔG, and the amino acid interactions [43,44].

3.2. Chemicals, Synthesis, and Characterizations

All of the reagents and solvents, as well as the memantine hydrochloride for biological evaluation and the chemicals needed for nervous tissue histology, were purchased from Sigma-Aldrich Química, S. de RL. de CV. (Toluca, Mexico). The synthesized *BZQuin* and Rlz were characterized using NMR and FT-Raman spectroscopic techniques. The NMR spectra (^{1}H, ^{13}C, and ^{11}B) were acquired with a Varian-Mercury NMR spectrometer operating at 300 MHz utilizing DMSO-d_6 as a solvent. All chemical shift values (δ) were reported in parts per million (ppm), using as reference the residual solvent peak and coupling constants, as (^{n}J) were in Hz. To indicate the multiplicity of the signals, the following abbreviations were used: *s* for a singlet; *d* for a doublet; *dd* for a doublet of doublets; and *m* for a multiplet (or different combinations of these). The Raman spectra were acquired with a Bruker-Senterra Neos9 FT-Raman microspectrophotometer with a laser at a wavelength of 785 nm at 100 mW.

3.2.1. Synthesis of 5-Oxo-2,2-diphenyl-[1,3,2]oxazaborolidine[3,4-a]pyridinium-6-carboxylic acid (*BZQuin*)

For the synthesis of *BZQuin*, 5 mmol of 2-aminoethyl diphenylborinate (2-APB) was suspended in 50 mL of a 5% *v*/*v* aqueous hydrochloric acid solution and stirred for 10 min to achieve hydrolysis. The resultant diphenylborinic acid was extracted with 60 mL of diethyl ether and was added to a suspension of 4.5 mmol of pyridine-2,3-dicarboxylic acid (quinolinic acid) in 30 mL of methanol; the mixture was stirred at −15 °C for 2.5 h. The solvent of the reaction mixture was evaporated under a vacuum, and the solid was recrystallized from an acetone/hexane/dichloromethane mixture (2:6:1). The *BZQuin* crystals were filtered and dried under a vacuum.

Analytical Data

5-Oxo-2,2-diphenyl-[1,3,2]oxazaborolidine[3,4-a]pyridinium-6-carboxylic acid (331.13 g/mol): yield of 87% and m.p. of 178-180°C. ^{1}H NMR (300 MHz, DMSO-d_6): δ 9.22 (*d*, J = 5.4 Hz, 1H), 8.70 (*d*, J = 7.6 Hz, 1H), 8.21 (*dd*, J = 7.7 Hz, 5.6 Hz, 1H), and 7.36–7.12 (*m*, 10H). ^{11}B NMR (96 MHz, DMSO): δ 9.05. ^{13}C NMR (75 MHz, DMSO-d_6): δ 165.27, 162.25, 144.21, 142.86, 138.17, 132.82, 132.26, 131.25, 129.80, 128.00, and 127.65. FT-Raman shift (wavenumber, cm^{-1}): 3050 (C-H$_{\nu(\text{stretch})}$), 2975 (O-H$_{\nu}$), 1747 (O=C-O-H$_{\nu}$), 1655 (O=C-O-B$_{\nu}$), 1594 (pyridine C=C$_{\nu}$), 1306 (C-H$_{\beta(\text{bending})}$), and 1001 (phenyl ring Breathing Mode).

3.2.2. Synthesis of 6-(Trifluoromethoxy)-1,3-benzothiazole-2-amine (Rlz)

For the synthesis of Rlz, 30 mmol of 4-(trifluoromethoxy) aniline was suspended with 85 mmol of ammonium thiocyanate and 35 mmol of potassium persulfate in 30 mL of a water/glacial acetic acid solution at a 1:10 ratio. The mixture was stirred at room temperature for 24 h and then at 40 °C for 2 additional h to complete the reaction. The resultant mixture was diluted with 60 mL of water/ethanol solution at a 5:1 ratio and was treated with 30% ammonium hydroxide until the pH was 12. The obtained suspension was filtered to obtain the raw product. Pure Rlz was obtained by the formation of its hydrochloric acid salt and later by recrystallization from an alkaline water/ethanol mixture (5:1). The Rlz crystals were filtered and dried under a vacuum.

Analytical Data

6-(Trifluoromethoxy)-1,3-benzothiazole-2-amine (234.20 g/mol): yield of 46% and m.p. of 118–119.5 °C. ^{1}H NMR (300 MHz, DMSO-d_6): δ 7.37 (*d*, J = 1.5 Hz, 1H), 7.27 (*s*, 2H), 6.98 (*d*, J = 8.7 Hz, 1H), and 6.78 (*dd*, J = 8.7 Hz, 1.5 Hz, 1H). ^{13}C NMR (75 MHz, DMSO-d_6): δ 167.81, 152.02, 142.17, 131.97, 125.43, 122.01, 119.04, 118.63, 118.00, and 114.51. FT-Raman shift (wavenumber, cm^{-1}): 3745 (N-H$_{2\nu}$), 3073 (C-H$_{\nu}$), 1270 (C-H$_{\beta}$), 715 (S-C$_{\nu}$), and 528 (N=C-S$_{\delta(\text{deformation})}$).

3.3. In Vivo Evaluation: Animals

For the *in vivo* biological evaluations, male CD-1 mice of 8–10 weeks old and 30–35 grams of weight were used. These were provided by the Vivarium at the Universidad Autónoma del Estado de Hidalgo. The animals were accommodated at the Biochemistry Research Laboratory of ESM-IPN under a normal day:night cycle without additional lights and under atmospheric conditions of temperature and humidity. They were housed in 48 × 37.5 × 21 cm polycarbonate boxes with stainless-steel grills as cover and pine sawdust as bedding, with food and water ad libitum. The mice were allowed to become acclimated to their new environment for 15 days prior to the experiments. The procedures were designed to comply with the current Mexican legislation in matters of the production, handling, care, and use of animals for research (NOM-062-ZOO-1999) and with the guidelines of the United States Food and Drug Administration (FDA). The experimental protocol was submitted to and approved by the Institutional Biosecurity Committee of ESM-IPN under code ESM-CBS-01/04-03-2021.

3.4. In Vivo Evaluation: Acute Toxicity

The acute toxicity of *BZQuin* was evaluated by the estimation of its LD_{50} amount with a modified version of Lorke's method and was compared to that of quinolinate. Eighteen mice were divided into six groups of three mice each ($n = 3$ per group). All administrations were intraperitoneal (i.p.) 0.5-mL injections using a 15% DMSO *v*/*v* solution as a vehicle; the effect of interest was death. In the first phase, three groups were administered with fixed doses of 10^1, 10^2, and 10^3 mg/kg, respectively. The mice were placed under the same previously described accommodation and housing conditions and were observed for 48 h in search of signs of toxic effects or death. After this, the surviving animals were euthanized for autopsy along with the corpses for the search of macroscopic signs of pathological changes. Considering the lethality results obtained from the first phase, three new doses based on quarters of logarithms were proposed for administering the three groups in the second phase. These were evaluated for complementing the data required for building the dose–response curve and for calculating *G*, considered as the LD_{50} amount of *BZQuin*. Likewise, after the administration of the second-phase doses, the mice were placed under the same accommodation and housing conditions, observed for 48 h, and subjected to autopsy [34,45]. The organization of the groups within phases is summarized in Table 2.

Table 2. Modified Lorke's method organization for estimating LD_{50}.

Modified Lorke's Method			
Phase I		**Phase II**	
Group	**Dose**	**Group**	**Dose**
1	10^1 mg/kg	1	$10^{0.25/1.25/2.25}$ mg/kg
2	10^2 mg/kg	2	$10^{0.50/1.50/2.50}$ mg/kg
3	10^3 mg/kg	3	$10^{0.75/1.75/2.75}$ mg/kg

3.5. In Vivo Evaluation: Murine Behavioral Model

For evaluating the effect of *BZQuin* on glutamatergic neurotransmission, a murine behavioral model was designed. In this in vivo model, the NMDA receptor agonist Quin and its derived boroxazolidone *BZQuin* were utilized as stimulating agents. Meanwhile, the antiglutamatergic and neuroprotective drugs Rlz and Mem were used as pretreatments for evaluating their ability to prevent effects related to Quin or *BZQuin* administration. Eighty mice were divided into ten groups ($n = 8$), and they were administered according to Table 3. For each mouse, the administrations of the Rlz and Mem pretreatments were carried out 10 and 60 min prior to the administration of the stimulating agent, respectively. This was performed to achieve their maximal concentration in the brain tissue during the experiment. The waiting time, along with the Rlz and Mem doses (10 mg/kg), was established considering the pharmacokinetic data available in the literature. The dose of Quin (300 mg/kg = 0.001795 mol/kg) as a stimulating agent was established based on toxicological studies of quinolinate and other kynurenines [35]. Meanwhile, for *BZQuin*, which is an unexplored compound, two doses were evaluated: one at a 1:1 molar ratio to that of Quin (593 mg/kg = 0.001795 mol/kg) and one below the estimated LD_{50} amount (100 mg/kg).

The evaluated *BZQuin* doses were established to compare its effect mole-by-mole against that of Quin and to observe its influence on behavior related to glutamatergic neurotransmission at a relatively safe dose. After the administration of the stimulating agents, there was a waiting time of 15 min before each mouse was subjected to the OFT for 10 min in a 50 × 50 × 50-cm Plexiglas box equipped with infrared beams. During this test, the number of times a mouse crossed an infrared beam was counted as the number of events and was considered a direct measure of the locomotor activity.

Table 3. Experimental design of the murine behavioral model.

Murine Behavioral Model		
Group	**Pretreatment**	**Stimulating Agent**
1	Vehicle (15% DMSO *v*/*v* with 0.9% *w*/*v* saline solution, intraperitoneal 0.5 mL injection)	None
2	Negative (vehicle, intraperitoneal 0.5 mL injection)	Quin (300 mg/kg, intraperitoneal 1 mL injection)
3	Rlz (riluzole 10 mg/kg, intraperitoneal 0.5 mL injection)	
4	Mem (memantine 10 mg/kg, subcutaneous 0.5 mL injection)	
5	Negative (vehicle, intraperitoneal 0.5 mL injection)	*BZQuin* (593 mg/kg, intraperitoneal 1 mL injection)
6	Rlz (riluzole 10 mg/kg, intraperitoneal 0.5 mL injection)	
7	Mem (memantine 10 mg/kg, subcutaneous 0.5 mL injection)	
8	Negative (vehicle, intraperitoneal 0.5 mL injection)	*BZQuin* (100 mg/kg, intraperitoneal 1 mL injection)
9	Rlz (riluzole 10 mg/kg, intraperitoneal 0.5 mL injection)	
10	Mem (memantine 10 mg/kg, subcutaneous 0.5 mL injection)	

Other parameters registered included the latency and intensity of seizures, which were classified according to a modified Racine scale suitable for seizures induced by iGluR agonists. After the OFT, the mice were maintained under observation under the same accommodation and housing conditions, and survival numbers at 48 h and 15 days were also registered [35,37,45–47].

3.6. Ex Vivo Evaluation: Nervous Tissue Histology

After the *in vivo* evaluation and once the 15 days of observation elapsed, two surviving mice from each group, together with two normal CD-1 mice, were selected for nervous tissue histology. During the latter, neuronal survival was evaluated in the brain sections.

Each mouse was euthanized with an i.p. injection of pentobarbital sodium at a dose of 60 mg/kg before its heart stopped beating. This was used as pump for tissue fixation. For this, 30 mL of PBS was administered directly into the left ventricle, while the vena cava was cut to displace the blood in the tissues. Immediately after this, 30 mL of 4% *w*/*v* paraformaldehyde aqueous solution was administered in the same way for fixating the tissues and preventing postmortem changes. Then, the corpses were decapitated, and the brains were extracted and stored in 10 mL of the same fixing agent solution. Before the brains were sectioned, they were dehydrated by submerging them in different ethanol aqueous solutions ranging from 70–96% *v*/*v* and, finally, in absolute 1-butanol. Once the dehydration process was completed, the brains were impregnated with Paraplast® and embedded in paraffin using a cubic mold. The brains embedded in the paraffin blocks were sectioned with a Leica RM2125RT microtome. The brain sections were made on the transverse plane, with a thickness of 7 μm and 2.5 mm above the beginning of the brainstem. This was carried out to observe the structures of interest, which included the ventral hippocampus, the striatum, and the brain and cerebellum cortexes. The sections were placed in a tissue water bath with gelatin at 41°C for their stretching and adhesion to the glass slides prior to histochemistry. The paraffin excess on each glass slide was removed with mild heating [48].

The histochemical technique used for staining the neurons was the Vogt method, which utilizes Cresyl violet as a dye for demonstrating basophilic bodies, such as the cell nuclei and the Nissl substance. For preparing the dye, a 2% *w*/*v* Cresyl violet acetate aqueous solution was prepared as stock. Then, 0.5 mL of this solution was added to 50 mL of acetate buffer (pH = 4.40) obtain the working solution. The staining procedure required the deparaffinization of the brain sections with xylenes prior to their being submerged, first in absolute ethanol and then in the working solution for 4 h. After the staining, the

excess dye was removed from the sections with 96% *v*/*v* ethanol aqueous solution; they were cleared with xylenes and mounted with synthetic resin. The slides were observed under a Nikon Eclipse E600 microscope; five different sections were observed (n = 5) for each group. In each of these, the neurons of the structures of interest were counted under a 20-× magnification objective in an area of 70,000 μm² [48,49].

3.7. Statistical Analysis

Throughout the analysis of the results, the Shapiro–Wilk normality test was used to determine whether the data of the various experiments had normal or non-normal distributions. For the experiments with normal distribution data, the statistical parametric tests employed were one-way ANOVA and two-way ANOVA, depending on the suitability of the data setup. For the experiments with non-normal distribution data, the statistical non-parametric test utilized was Kruskal–Wallis. After each statistical test, the post hoc test employed for comparisons was Tukey. For some results, such as those of locomotor activity, parametric and non-parametric tests were utilized for analyzing the data depending on the groups considered, in that this affected normality. In the nervous tissue histology, the experimental data considering all the groups were not suitable for a two-way ANOVA. Therefore, a one-way ANOVA was carried out instead for comparing the normal and vehicle groups against the others. Then, the normal and vehicle groups were obviated, and a two-way ANOVA was performed to compare the groups with pharmacologic treatment against each other to assess the influence that each factor exerted on neuron survival. In Supplementary Table S7, the LSM of the neuron counts and SEMs for the pretreatments and stimulating agents are shown, and these were used for global comparisons. Meanwhile, in Supplementary Table S8, the LSM of the neuron counts and SEMs for the interactions are shown, and these were used for simple comparisons.

4. Conclusions

In this work, quinolinate and its intrinsic biological effects were used as the starting point for the design and synthesis of an organoboron compound named *BZQuin* with the purpose of influencing neurotransmission in the CNS. Based on the results of the in silico, in vivo, and ex vivo evaluations, it could be concluded that *BZQuin* exerted a positive influence on glutamatergic neurotransmission. This latter was suggested to be related to its direct interaction with the mGluR1, mGluR2, and mGluR7 receptors. This could be affirmed based on the in vivo results obtained: higher locomotor activity, longer latency time, and lower seizure intensity among the groups administered with *BZQuin* were indicative of the positive, but relatively slow, influence of this compound on neurotransmission. The neurotoxicity observed in the neuron counts of these same groups was indicative that the observed effect was somehow related to glutamatergic neurotransmission and excitotoxicity. The involvement of glutamatergic neurotransmission in the observed *BZQuin* effects was further supported by the fact that Rlz and Mem, both antiglutamatergic and neuroprotective drugs, prevented the occurrence of the majority of *BZQuin* effects observed in the *in vivo* and *ex vivo* evaluations. The targets for *BZQuin*, the metabotropic glutamate receptors mGluR1, mGluR2, and mGluR7, were proposed based on the *in silico* results of molecular docking, as these results suggested their binding. These results were complementary to the *ex vivo* results. In the latter, the glutamatergic neurotoxic *BZQuin* effect was selective for certain areas in the studied neuroanatomical structures, with reported high expressions of the previously mentioned mGluRs. Additionally, the slow, positive influence on neurotransmission observed in the in vivo experiments may be due to *BZQuin*'s interactions with mGluRs; these acted through mechanisms that were slower than iGluRs or other ionic channels. All of the results complemented each other to suggest the glutamatergic effect of *BZQuin*.

Additional experiments must be carried out to support selectivity among mGluRs and to suggest a therapeutic dose, despite the results indicating that *BZQuin* is bioactive and safe below 100 mg/kg. In addition, these experiments must be conducted to determine

a dose at which the stimulant effects of *BZQuin* no longer appear to turn into excitotoxicity or border with it. In addition, experimental confirmation of *BZQuin* interactions with its possible target mGluRs can be assessed by radioligand-binding assays or protein crystallography, among other methods. Considering all of the results, the present article contributes to the innovative synthesis [50,51] and to the search of novel possible pharmacological applications for organoboron compounds [21,52–54].

Supplementary Materials: The following supporting information can be downloaded at: https://www.mdpi.com/article/10.3390/inorganics11030094/s1, Figure S1: BOILED-Egg graph for BZQuin, Quin, L-glutamate, and D-aspartate; Figure S2: Mice survival at 2 and 15 days; Figure S3-S7: ^{1}H, ^{13}C and ^{11}B NMR spectra of BZQuin. Figure S8: HETCOR 2D NMR experiment for BZQuin. Figure S9. Raman spectrum of BZQuin. Figure S10-S13: ^{1}H and ^{13}C NMR spectra of Rlz. Figure S14: HETCOR 2D NMR experiment for RLZ; Figure S15. Raman spectrum of Rlz. Table S1: Predicted cytochrome inhibition and Lipinski's Rule of Five; Table S2: Gibbs energies and binding probabilities; Table S3. Modified Lorke's method results; Table S4. Global comparisons of locomotor activity; Table S5. Simple comparisons of locomotor activity; Table S6. Seizure intensity comparison. Table S7. Global comparisons of neuron counts. Table S8. Simple comparisons of neuron counts.

Author Contributions: Conceptualization, M.E.C.-G., M.A.S.-U. and J.G.T.-F.; methodology, M.E.C.-G., B.A.R.-V., I.I.P.-M. and R.A.J.-L.; software, M.E.C.-G.; validation, R.A.J.-L., M.A.S.-U. and J.G.T.-F.; formal analysis, M.E.C.-G. and B.A.R.-V.; investigation, M.E.C.-G.; resources, R.A.J.-L., I.I.P.-M., M.A.S.-U. and J.G.T.-F.; data curation, M.E.C.-G. and B.A.R.-V.; writing—original draft preparation, M.E.C.-G.; writing—review and editing, M.E.C.-G., M.A.S.-U. and J.G.T.-F.; visualization, M.E.C.-G.; supervision, M.A.S.-U. and J.G.T.-F.; project administration, J.G.T.-F., and funding acquisition, M.E.C.-G., M.A.S.-U. and J.G.T.-F.. All authors have read and agreed to the published version of the manuscript.

Funding: The authors would like to thank the Consejo Nacional de Ciencia y Tecnología (CONACyT) for the scholarship granted under CVU number 744662 and the IPN program "Beca de estímulo institucional de formación de investigadores" for the scholarships granted under registry numbers 2025, 425, and 580. Additionally, the authors thank the *Secretaría de Investigación y Posgrado del Instituto Politécnico Nacional* for financial support of this project (grant: M-2143).

Data Availability Statement: All data, including output files for analyzing the docking results are available by requesting to corresponding authors.

Acknowledgments: The authors would like to thank Maggie Brunner for checking the appropriate use of the English language in this manuscript.

Conflicts of Interest: The authors declare no conflict of interest.

References

1. Marmiroli, P.; Cavaletti, G. The Glutamatergic Neurotransmission in the Central Nervous System. *Curr. Med. Chem.* **2012**, *19*, 1269–1276.
2. Niciu, M.J.; Kelmendi, B.; Sanacora, G. Overview of Glutamatergic Neurotransmission in the Nervous System. *Pharmacol. Biochem. Behav.* **2012**, *100*, 656–664.
3. Bashir, Z.I.; Bortolotto, Z.A.; Davies, C.H.; Berretta, N.; Irving, A.J.; Seal, A.J.; Henley, J.M.; Jane, D.E.; Watkins, J.C.; Collingridge, G.L. Induction of LTP in the Hippocampus Needs Synaptic Activation of Glutamate Metabotropic Receptors. *Nature* **1993**, *363*, 347–350.
4. Stahl, S.M. *Stahl's Essential Psychopharmacology: Neuroscientific Basis and Practical Applications*; Cambridge University Press: Cambridge, UK, 2021; ISBN 1108981216.
5. Cheah, B.C.; Vucic, S.; Krishnan, A.; Kiernan, M.C. Riluzole, Neuroprotection and Amyotrophic Lateral Sclerosis. *Curr. Med. Chem.* **2010**, *17*, 1942–1959.
6. Olney, J.W. Excitotoxic Amino Acids: Research Applications and Safety Implications. In: Glutamic Acid Advances in Biochemistry and Physiology 1 ed. Lloyd J. Filer Eds; Raven Press: New York, NY, USA **1979**, *pp.* 287–319.
7. Heath, P.R.; Shaw, P.J. Update on the Glutamatergic Neurotransmitter System and the Role of Excitotoxicity in Amyotrophic Lateral Sclerosis. *Muscle Nerve Off. J. Am. Assoc. Electrodiagn. Med.* **2002**, *26*, 438–458.
8. Lapin, I.P. Kynurenines and Seizures. *Epilepsia* **1981**, *22*, 257–265.

9. HEYES, M.P.; Saito, K.; Crowley, J.S.; Davis, L.E.; Demitrack, M.A.; Der, M.; Dilling, L.A.; Elia, J.; Kruesi, M.J.P.; Lackner, A. Quinolinic Acid and Kynurenine Pathway Metabolism in Inflammatory and Non-Inflammatory Neurological Disease. *Brain* **1992**, *115*, 1249–1273.
10. Stone, T.W. Kynurenic Acid Antagonists and Kynurenine Pathway Inhibitors. *Expert Opin. Investig. Drugs* **2001**, *10*, 633–645.
11. Esquivel, D.G.; Ramirez-Ortega, D.; Pineda, B.; Castro, N.; Rios, C.; de la Cruz, V.P. Kynurenine Pathway Metabolites and Enzymes Involved in Redox Reactions. *Neuropharmacology* **2017**, *112*, 331–345.
12. Fazio, F.; Lionetto, L.; Curto, M.; Iacovelli, L.; Copeland, C.S.; Neale, S.A.; Bruno, V.; Battaglia, G.; Salt, T.E.; Nicoletti, F. Cinnabarinic Acid and Xanthurenic Acid: Two Kynurenine Metabolites That Interact with Metabotropic Glutamate Receptors. *Neuropharmacology* **2017**, *112*, 365–372.
13. Lovelace, M.D.; Varney, B.; Sundaram, G.; Franco, N.F.; Ng, M.L.; Pai, S.; Lim, C.K.; Guillemin, G.J.; Brew, B.J. Current Evidence for a Role of the Kynurenine Pathway of Tryptophan Metabolism in Multiple Sclerosis. *Front. Immunol.* **2016**, *7*, 246.
14. Guillemin, G.J. Quinolinic Acid, the Inescapable Neurotoxin. *FEBS J.* **2012**, *279*, 1356–1365.
15. Guillemin, G.J.; Wang, L.; Brew, B.J. Quinolinic Acid Selectively Induces Apoptosis of Human Astrocytes: Potential Role in AIDS Dementia Complex. *J. Neuroinflammation* **2005**, *2*, 16.
16. Guillemin, G.J.; Meininger, V.; Brew, B.J. Implications for the Kynurenine Pathway and Quinolinic Acid in Amyotrophic Lateral Sclerosis. *Neurodegener. Dis.* **2005**, *2*, 166–176.
17. Tang, J.; Zheng, X.; Xiao, K.; Wang, K.; Wang, J.; Wang, Y.; Wang, K.; Wang, W.; Lu, S.; Yang, K. Effect of Boric Acid Supplementation on the Expression of BDNF in African Ostrich Chick Brain. *Biol. Trace Elem. Res.* **2016**, *170*, 208–215.
18. Pizzorno, L. Nothing Boring about Boron. *Integr. Med. A Clin. J.* **2015**, *14*, 35.
19. Farfán-García, E.D.; Castillo-Mendieta, N.T.; Ciprés-Flores, F.J.; Padilla-Martínez, I.I.; Trujillo-Ferrara, J.G.; Soriano-Ursúa, M.A. Current Data Regarding the Structure-Toxicity Relationship of Boron-Containing Compounds. *Toxicol. Lett.* **2016**, *258*, 115–125.
20. Abdelnour, S.A.; Abd El-Hack, M.E.; Swelum, A.A.; Perillo, A.; Losacco, C. The Vital Roles of Boron in Animal Health and Production: A Comprehensive Review. *J. Trace Elem. Med. Biol.* **2018**, *50*, 296–304.
21. Barrón-González, M.; Montes-Aparicio, A.; Cuevas-Galindo, M.E.; Orozco-Suárez, S.; Barrientos, R.; Alatorre, A.; Querejeta, E.; Trujillo-Ferrara, J.G.; Farfán-García, E.D.; Soriano-Ursúa, M.A. Boron-Containing Compounds on Neurons: Actions and Potential Applications for Treating Neurodegenerative Diseases. *J. Inorg. Biochem.* **2022**, *238*, 112027.
22. Franckowiak, R.; Peterschmitt, L. La Chimie de Homberg: Une Vérité Certaine Dans Une Physique Contestable. *Early Sci. Med.* **2005**, *10*, 65–90.
23. Rosalez, M.N.; Estevez-Fregoso, E.; Alatorre, A.; Abad-García, A.; A Soriano-Ursúa, M. 2-Aminoethyldiphenyl Borinate: A Multitarget Compound with Potential as a Drug Precursor. *Curr. Mol. Pharm.* **2020**, *13*, 57–75.
24. Ozaki, S.; Suzuki, A.Z.; Bauer, P.O.; Ebisui, E.; Mikoshiba, K. 2-Aminoethyl Diphenylborinate (2-APB) Analogues: Regulation of Ca2+ Signaling. *Biochem. Biophys. Res. Commun.* **2013**, *441*, 286–290.
25. Araujo-Alvarez, J.M.; Trujillo-Ferrara, J.G.; Ponce-Franco, D.; Correa-Basurto, J.; Delgado, A.; Querejeta, E. (+)-(S)-trujillon,(+)-(S)-4-(2, 2-diphenyl-1, 3, 2-oxazabolidin-5-oxo) Propionic Acid, a Novel Glutamatergic Analog, Modifies the Activity of Globus Pallidus Neurons by Selective NMDA Receptor Activation. *Chirality* **2011**, *23*, 429–437.
26. Abad-García, A.; Ocampo-Néstor, A.L.; Das, B.C.; Farfán-García, E.D.; Bello, M.; Trujillo-Ferrara, J.G.; Soriano-Ursúa, M.A. Interactions of a Boron-Containing Levodopa Derivative on D2 Dopamine Receptor and Its Effects in a Parkinson Disease Model. *JBIC J. Biol. Inorg. Chem.* **2022**, *27*, 121–131.
27. Barrón-González, M.; Rosales-Hernández, M.C.; Abad-García, A.; Ocampo-Néstor, A.L.; Santiago-Quintana, J.M.; Pérez-Capistran, T.; Trujillo-Ferrara, J.G.; Padilla-Martínez, I.I.; Farfán-García, E.D.; Soriano-Ursúa, M.A. Synthesis, In Silico, and Biological Evaluation of a Borinic Tryptophan-Derivative That Induces Melatonin-like Amelioration of Cognitive Deficit in Male Rat. *Int. J. Mol. Sci.* **2022**, *23*, 3229.
28. Daina, A.; Michielin, O.; Zoete, V. SwissADME: A Free Web Tool to Evaluate Pharmacokinetics, Drug-Likeness and Medicinal Chemistry Friendliness of Small Molecules. *Sci. Rep.* **2017**, *7*, 42717.
29. Daina, A.; Zoete, V. A Boiled-egg to Predict Gastrointestinal Absorption and Brain Penetration of Small Molecules. *ChemMedChem* **2016**, *11*, 1117–1121.
30. Dobrovetsky, E.; Khutoreskaya, G.; Seitova, A.; Cossar, D.; Edwards, A.M.; Arrowsmith, C.H.; Bountra, C.; Weigelt, J.; Bochkarev, A.; Consortium, S.G. Metabotropic Glutamate Receptor Mglur1 Complexed with LY341495 Antagonist. **2010**. Doi: 10.2210/pdb3ks9/pdb. Available at: https://www.rcsb.org/structure/3ks9.
31. Monn, J.A.; Prieto, L.; Taboada, L.; Hao, J.; Reinhard, M.R.; Henry, S.S.; Beadle, C.D.; Walton, L.; Man, T.; Rudyk, H. Synthesis and Pharmacological Characterization of C 4-(Thiotriazolyl)-Substituted-2-Aminobicyclo [3.1. 0] Hexane-2, 6-Dicarboxylates. Identification of (1 R, 2 S, 4 R, 5 R, 6 R)-2-Amino-4-(1 H-1, 2, 4-Triazol-3-Ylsulfanyl) Bicyclo [3.1. 0] Hexane-2, 6-Dicarboxylic Acid (LY2812223), a Highly Potent, Functionally Selective MGlu2 Receptor Agonist. *J. Med. Chem.* **2015**, *58*, 7526–7548.
32. Çolak, A.T.; Şahin, Y.; Yeşilel, O.Z.; Çolak, F.; Yılmaz, F.; Taş, M. Novel Boron Compounds of 2, 3-and 2, 5-Pyridinedicarboxylic Acids. *Inorg. Chim. Acta* **2012**, *383*, 169–177.
33. Trujillo, J.; Höpfl, H.; Castillo, D.; Santillan, R.; Farfán, N. X-Ray Crystallographic Study of Boroxazolidones Obtained from L-Ornithine, L-Methionine, Kainic Acid and 2, 6-Pyridinedicarboxylic Acid. *J. Organomet. Chem.* **1998**, *571*, 21–29.
34. Lorke, D. A New Approach to Practical Acute Toxicity Testing. *Arch. Toxicol.* **1983**, *54*, 275–287.
35. Lapin, I.P. Stimulant and Convulsive Effects of Kynurenines Injected into Brain Ventricles in Mice. *J. Neural Transm.* **1978**, *42*, 37–43.

36. Brunton, L.L.; Chabner, B.A.; Knollmann, B.C. *Goodman & Gilman: The pharmacological basis of therapeutics*; McGraw Hill: New York, NY, USA, 2019; ISBN 1259584739.
37. Sharma, S.; Puttachary, S.; Thippeswamy, A.; Kanthasamy, A.G.; Thippeswamy, T. Status Epilepticus: Behavioral and Electroencephalography Seizure Correlates in Kainate Experimental Models. *Front. Neurol.* **2018**, *9*, 7.
38. Shigemoto, R.; Kinoshita, A.; Wada, E.; Nomura, S.; Ohishi, H.; Takada, M.; Flor, P.J.; Neki, A.; Abe, T.; Nakanishi, S. Differential Presynaptic Localization of Metabotropic Glutamate Receptor Subtypes in the Rat Hippocampus. *J. Neurosci.* **1997**, *17*, 7503–7522.
39. Paquet, M.; Smith, Y. Group I Metabotropic Glutamate Receptors in the Monkey Striatum: Subsynaptic Association with Glutamatergic and Dopaminergic Afferents. *J. Neurosci.* **2003**, *23*, 7659–7669.
40. Sherman, S.M. The Function of Metabotropic Glutamate Receptors in Thalamus and Cortex. *Neurosci.* **2014**, *20*, 136–149.
41. Yuzaki, M.; Mikoshiba, K. Pharmacological and Immunocytochemical Characterization of Metabotropic Glutamate Receptors in Cultured Purkinje Cells. *J. Neurosci.* **1992**, *12*, 4253–4263.
42. Tempia, F.; Miniaci, M.C.; Anchisi, D.; Strata, P. Postsynaptic Current Mediated by Metabotropic Glutamate Receptors in Cerebellar Purkinje Cells. *J Neurophysiol.* **1998**, *80*, 520–528.
43. Foresman, J.; Frish, E. *Exploring Chemistry*; Gaussian Inc.: Pittsburg, CA, USA, 1996.
44. Trott, O.; Olson, A.J. AutoDock Vina: Improving the Speed and Accuracy of Docking with a New Scoring Function, Efficient Optimization, and Multithreading. *J. Comput. Chem.* **2010**, *31*, 455–461.
45. Gad, S.C.; Cassidy, C.D.; Aubert, N.; Spainhour, B.; Robbe, H. Nonclinical Vehicle Use in Studies by Multiple Routes in Multiple Species. *Int. J. Toxicol.* **2006**, *25*, 499–521.
46. Milane, A.; Tortolano, L.; Fernandez, C.; Bensimon, G.; Meininger, V.; Farinotti, R. Brain and Plasma Riluzole Pharmacokinetics: Effect of Minocycline Combination. *J. Pharm. Pharm. Sci.* **2009**, *12*, 209–217.
47. Beconi, M.G.; Howland, D.; Park, L.; Lyons, K.; Giuliano, J.; Dominguez, C.; Munoz-Sanjuan, I.; Pacifici, R. Pharmacokinetics of Memantine in Rats and Mice. *PLoS Curr.* **2011**, *3*, RRN1291.
48. Gridley, M.F. *Manual of Histologic and Special Staining Technics*; Armed Forces Institute of Pathology: Dhaka, Bangladesh, 1957.
49. Alvarez-Buylla, A.; Ling, C.-Y.; Kirn, J.R. Cresyl Violet: A Red Fluorescent Nissl Stain. *J. Neurosci. Methods* **1990**, *33*, 129–133.
50. Das, B.C.; Nandwana, N.K.; P.Ojha, D.; Das, S.; Evans, T. Synthesis of a boron-containing amidoxime reagent and its application to synthesize functionalized oxadiazole and quinazolinone derivatives. *Tetrahedron Lett.* **2022**, *92*, 153657.
51. Saito, Y.; Yoshida, N.; Nakagawa-Goto, K. Boroxazolidone Formation under Physiological Conditions as a Tool for the Chemical Modification of Biomolecules. *Chem. Lett.* **2021**, *50*, 1695–1698.
52. Di Battista, V.; Hey-Hawkins, E. Development of Prodrugs for Treatment of Parkinson's Disease: New Inorganic Scaffolds for Blood–Brain Barrier Permeation. *J. Pharm. Sci.* **2022**, *111*, 1262–1279.
53. Gruzdev, D.A.; Telegina, A.A.; Levit, G.L.; Krasnov, V.P. N-Aminoacyl-3-amino-nido-carboranes as a Group of Boron-Containing Derivatives of Natural Amino Acids. *J. Org. Chem.* **2022**, *87*, 5437–5441, doi:10.1021/acs.joc.2c00151.
54. Imperio, D.; Panza, L. Sweet Boron: Boron-Containing Sugar Derivatives as Potential Agents for Boron Neutron Capture Therapy. *Symmetry* **2022**, *14*, 182.